Congenital Blindness affects Diencephalic but not Mesencephalic Structures in the Human Brain

Luca Cecchetti[1,2], Emiliano Ricciardi[1], Giacomo Handjaras[1,2], Ron Kupers[3], Maurice Ptito[3,4,5] and Pietro Pietrini[1,2]

1 - Laboratory of Clinical Biochemistry and Molecular Biology, Department of Surgery, Medical and Molecular Pathology, and Critical Care, University of Pisa, Pisa, Italy;
2 - Clinical Psychology Branch, Pisa University Hospital, Pisa, Italy;
3 - BRAINlab and Neuropsychiatry Laboratory, Department of Neuroscience & Pharmacology, Panum Institute, University of Copenhagen, Copenhagen, Denmark;
4 - Harland Sanders Chair, School of Optometry, University of Montreal, Montreal, Canada;
5 - Laboratory of Neuropsychiatry, Psychiatric Centre Copenhagen and Department of Neuroscience and Pharmacology, University of Copenhagen, Copenhagen, Denmark;

Running Title: The subcortical blind brain

Correspondence to:
Emiliano Ricciardi
Laboratory of Clinical Biochemistry and Molecular Biology
Department of Surgery, Medical and Molecular Pathology, and Critical Care
University of Pisa
Building 43, Via Savi 10, 56126, Pisa, Italy
E-mail: emiliano.ricciardi@bioclinica.unipi.it

Abstract

While there is ample evidence that the structure and function of visual cortical areas are affected by early visual deprivation, little is known of how early blindness modifies sub-cortical relay and association thalamic nuclei, as well as mesencephalic structures. Therefore, we used MRI in a multicenter study to measure volume of thalamic nuclei relaying sensory and motor information to the neocortex, parcellated according to atlas-based thalamo-cortical connections, and in the superior and inferior colliculi, in 29 individuals with congenitally blindness of peripheral origin (17M; age: 35.7 ± 14.3 years) and 29 sighted subjects (17M; age: 31.9 ± 9.0). Blind participants showed an overall volume reduction in the left [$p = 0.008$] and right [$p = 0.007$] thalami, as compared to the sighted individuals. Specifically, the lateral geniculate (i.e., primary visual thalamic relay nucleus) was 40% reduced [left: $p = 4\times10^{-6}$; right: $p < 1\times10^{-6}$], consistent with findings from animal studies. In addition, association thalamic nuclei projecting to temporal [left: $p = 0.005$; right: $p = 0.005$], prefrontal [left: $p = 0.010$; right: $p = 0.014$], occipital [left: $p = 0.005$; right: $p = 0.023$] and right premotor [$p = 0.024$] cortical regions were also significantly reduced in the congenitally blind group. Conversely, volumes of the relay nuclei directly involved in auditory, motor and somatosensory processing were not affected by visual deprivation. In contrast, no difference in volume was observed in either the superior or the inferior colliculus between the two groups.

Our findings indicate that visual loss since birth leads to selective volumetric changes within diencephalic, but not mesencephalic, structures. Both changes in reciprocal cortico-thalamic connections or modifications in the intrinsic connectivity

between relay and association nuclei of the thalamus may contribute to explain these alterations in thalamic volumes. Sparing of the superior colliculi is in line with their composite, multisensory projections and with their not exclusive visual nature.

Keywords: Thalamus; Superior colliculus; Lateral geniculate nucleus; Congenital blindness; Morphometry;

Introduction

Among sensory modalities, vision has a key-role in defining how humans acquire knowledge and interact with the surrounding world. From more 'perceptual' tasks such as spatial localization, shape, size and depth discrimination, to more 'cognitive' tasks, including object recognition or social interaction, human behavior, and that of non-human primates, is highly influenced by the strong reliance on vision (Pavani et al., 2000; Ehrsson, 2007). In addition, the importance of the visual modality is reflected not only by the number of sub-cortical structures involved but also by the large proportion of the neocortical surface dedicated to the processing of visual stimuli (Felleman and Van Essen, 1991). Unsurprisingly, loss of vision leads to 'plastic' adaptive modifications in the structural and functional architecture of the 'visual' brain, especially when blindness onset occurs at birth or at an early stage of life (Berardi et al., 2000; Karlen et al., 2006). Indeed, several studies in both early and late blind individuals reported atrophy in grey and white matter structures of the 'visual' pathway, affecting the optic nerves, chiasm and radiations, lateral geniculate nucleus, pulvinar, splenium of corpus callosum, as well as striate and extrastriate visual cortical areas (Noppeney et al., 2005; Shimony et al., 2006; Pan et al., 2007; Ptito et al., 2008; Shu et al., 2009; Shu et al., 2009a; Leporé et al., 2010; Tomaiuolo et al., 2014; Wang et al., 2014). In contrast, other studies demonstrated that early blind individuals retain a normally developed stria of Gennari (Trampel et al., 2011). Other alterations include an increased cortical thickness in the occipital pole (Bridge

et al., 2009; Jiang et al., 2009; Park et al., 2009) and modified cortico-cortical connectivity patterns (Klinge et al., 2010; Collignon et al., 2013; Ioannides et al., 2013). Furthermore, blind individuals activate 'visual' cortical areas when performing a variety of non-visual perceptual and cognitive tasks (Pietrini et al., 2004; Ptito and Desgent, 2006; Noppeney, 2007; Bonino et al., 2008; Cattaneo et al., 2008; Ricciardi et al., 2009; Merabet and Pascual-Leone, 2010; Kupers et al., 2011; Kupers and Ptito, 2014) and this recruitment is due to two distinct brain processes. First, a large extent of the brain structural and functional cortical architecture develops also in the absence of any visual experience and is able to process information independently from the sensory modality through which it has been acquired - a property named *supramodality* - both in sighted and sensory-deprived individuals (Pietrini et al., 2004; Ricciardi et al., 2007; Ricciardi et al., 2009, 2013, 2014; Ricciardi and Pietrini, 2011). Second, visual experience does shape cortical brain development. Therefore, loss of sight, especially at birth or in the early phases of life, and the consequent recruitment of the occipital cortex by alternate sensory/cognitive functions, may be specifically related to a widespread crossmodal plastic rearrangement of connectivity patterns that extends well beyond (the usual limits of) vision-related cortical structures (Ricciardi and Pietrini, 2011; Kupers and Ptito, 2014; Qin et al., 2014; Ricciardi et al., 2014).

Several findings challenged the hypothesis that structural and functional brain modifications in early blindness predominantly involve the neocortex (Bavelier and Neville, 2002; Bridge et al., 2009), and demonstrated rather that congenital blindness also affects certain subcortical structures, not directly involved in visual perception. For instance, the volume of the posterior portion of the right hippocampus is reduced in congenital blindness (Chebat et al., 2007, Leporé et al., 2009), while its anterior

portion is enlarged (Fortin et al., 2008). Further sub-cortical modifications occur in the putamen (Bridge et al., 2009) and the cortico-spinal tract of blind subjects (Yu et al., 2007).

During development, subcortical regions are shaped by sensory inputs (Sur et al., 1988), and their cortical projections have a relevant role determining the functional architecture of the whole brain (Frost et al., 2000; Sharma et al., 2000; Von Melchner et al., 2000). In the absence of visual input from birth, the development of subcortical structures mainly involved in non-visual processing can take an alternative trajectory. For example, bilateral enucleation in short-tailed opossums alters the overall volume of subcortical regions like the thalamus, the midbrain and the rhombencephalon (Karlen and Krubitzer, 2009; Desgent and Ptito, 2012). Amongst these structures, the thalamus plays an important part in sensory processing and integration, given its key position in establishing input–output connections between multiple sensory and motor cortical areas (Cappe et al., 2009). In conditions of early visual deprivation, reorganization of the interconnections between thalamic nuclei and the whole thalamo-cortical projection network can occur (Sur et al., 1988; Ghazanfar and Schroeder, 2006), leading to functional and morphometric alterations of specific thalamic subregions in the adult. A vast literature in animal models of visual deprivation has described the alterations that occur in the architecture of the metathalamus, which comprises the lateral and medial geniculate bodies (Sakakura and Iwama, 1967; Headon and Powell, 1973; Cullen and Kaiserman-Abramof, 1976; Desgent and Ptito, 2012). In sharp contrast to the abundance of animal studies, only a few studies on visual deprivation in humans with congenital anophthalmia (Bridge et al., 2009) or acquired glaucoma (Gupta et al., 2009; Chen et al., 2013; Lee et al.,

2014) have reported structural changes in the metathalamic nuclei, but none of them examined potential modifications in thalamic subregions.

Another important structure involved in visual processing is the superior colliculus, a phylogenetically ancient laminated structure (Hilbig et al., 1999; White and Munoz, 2011) that, together with the inferior colliculus, constitutes the mesencephalic tectum. In human and in non-human primates, similarly to other mammals, the most superficial strata of the superior colliculus receive direct retinal inputs (Tiao and Blackmore, 1976; Wallace et al., 1996; May, 2006) and project to striate and extrastriate visual areas (White and Munoz, 2011). Therefore, the retinotectal system is considered to be part of the visual pathway. Although the superior colliculus is retinotopically organized (DuBois and Cohen, 2000; Sylvester et al., 2007; Limbrick-Oldfield et al., 2012), it also contributes to visual perception without awareness (Leh et al., 2006; Leh et al., 2010) and to spatial attention (Schneider and Kastner, 2009; Katyal et al., 2010); its deeper layers are involved in saccades and gaze control (Krebs et al., 2010), as well as in multisensory integration (Sparks and Hartswitch-Young, 1989; Wallace and Stein, 1994; Burnett et al., 2004).

To our knowledge, only a few studies investigated the structure of the human mesencephalic tectum by means of in-vivo techniques, and particularly focused on the changes induced by neoplastic (Sherman et al., 1987) and neurodegenerative diseases (Masucci et al., 1995; Warmuth-Metz et al., 2001). While some animal studies reported dramatic volumetric and cytoarchitectonic modifications in the superior colliculus of enucleated (Lund and Lund 1971; Rhoades, 1980; Smith and Bedi, 1997) and genetically blind rodents (Crish et al., 2006), a study on unilateral cortical blindness following hemispherectomy in the monkey showed that the superior colliculus retained its functionality, despite a notable volume reduction (Théoret et

al., 2001). Most importantly, to date there are no studies that have investigated the effects of visual deprivation since birth on the human superior colliculus.

Here, by using a multicenter sample of congenitally blind subjects and in-vivo MR imaging, we assessed whether lack of sight since birth causes volumetric and morphometric changes within the thalamic nuclei or the mesencephalic tectum. In particular, we defined the specific volumetric changes of thalamic subregions relaying sensory and motor information to the neocortex, parcellated according to atlas-based thalamo-cortical connections. Thalamic nuclei projecting to the temporal, prefrontal and occipital cortical regions were altered in congenital blind subjects, as compared to a matched sighted cohort. On the other hand, thalamic nuclei projecting to posterior parietal, auditory, somatosensory and motor cortices, as well as the superior and inferior colliculi were not affected by the absence of sight.

Materials & Methods

Subjects

Twenty-nine congenitally blind (CB; 17 M; age: 35.7 ± 14.3 years) and 29 sighted control subjects (SC; 17 M; age: 31.9 ± 9.0 years) recruited at three different research centers (Laboratory of Clinical Biochemistry and Molecular Biology in Pisa, Italy; BRAINlab in Copenhagen, Denmark; School of Optometry in Montreal, Canada) participated in the study. Specifically, 11 CB and 11 SC belonged to the Italian, 10 CB and 10 SC to the Danish, and 8 CB and 8 SC to the Canadian sample. There were no age differences between sighted and blind subjects [$t(56) = 1.20$, $p = 0.24$]. Causes of blindness are summarized in Table 1. All subjects were blind since birth.

All participants underwent a medical examination in order to exclude history or presence of any medical, neurological and/or psychiatric disorder, other than blindness in the CB, that could affect brain morphology or function and gave their written informed consent after the study procedures and the risks involved had been explained. The Institutional Ethics Committee of each respective research center approved the protocol and the study was conducted in accordance to the Declaration of Helsinki.

Table 1 about here

MR acquisition

Italian participants were scanned using a 1.5 Tesla GE Signa Excite magnet; for each participant, a three-dimensional fast spoiled gradient recall (3D-FSPGR) T1 was

collected as follows: repetition time (TR) = 2270 ms; echo time (TE) = 3.6 ms; flip angle (FA) = 10°; field of view (FOV) = 240 x 240 mm; acquisition matrix = 512 x 512; in-plane resolution = 0.47 x 0.47 mm; slice thickness = 1 mm; 150 axial slices. The obtained images were then resampled to a 1 x 1 x 1 mm resolution, in order to match the voxel dimensions of the other two samples involved in the study. Danish participants were scanned using a 3 Tesla Siemens Trio scanner with the following parameters: 3D-MPRAGE T1; TR = 1540 ms; TE = 3.9 ms; FA = 30°; FOV = 256 x 256 mm; acquisition matrix = 256 x 256; in-plane resolution = 1 x 1 mm; slice thickness = 1 mm; 192 sagittal slices. For the Canadian volunteers, structural images of the brain were collected on a 1.5 Tesla Siemens Magnetom Avanto scanner (3D-MPRAGE T1; TR = 2240 ms; TE = 9.2 ms; FA = 10° FOV = 256 x 256 mm; acquisition matrix = 256 × 256, in-plane resolution = 1x 1 mm; slice thickness = 1 mm; 160 sagittal slices).

Data Analysis

Data analysis was carried out using ROBEX v1.2 (http://www.nitrc.org/projects/robex), SPM v8.0 (http://www.fil.ion.ucl.ac.uk/spm/), FSL tools -FMRIB Software Library v5.0 (Smith et al., 2004; Jenkinson et al., 2012; http://fsl.fmrib.ox.ac.uk/fsl/fslwiki/FSL), Caret v5.65 (Van Essen et al., 2001; http://www.nitrc.org/projects/caret/), 3dViewer plugin for ImageJ (Schmid et al., 2010; http://3dviewer.neurofly.de/), MathWorks MATLAB Release 2012a (http://www.mathworks.com/products/matlab/), and IBM SPSS v21.0.0 (http://www-01.ibm.com/software/uk/analytics/spss/).

In the common preprocessing for all the further analysis, MRI acquisitions were brain-extracted using ROBEX (Iglesias et al., 2011), an automatic algorithm that robustly removes non-brain tissues from T1-weighted scan, so as to ensure the stability/robustness of subsequent critical steps in the analysis pipeline, such as the spatial transformation in the standard space and tissue type segmentation (Iglesias et al., 2011).

Global and Local Volume Estimation of the Thalamus

The open source software package FSL v5.0 was adopted as a tool to accurately estimate the effects of congenital blindness on visual and non-visual thalamic nuclei volumes. Specifically, brain extracted MR images were segmented into white matter (WM), grey matter (GM) and cerebrospinal fluid (CSF) and corrected for radiofrequency pulse inhomogeneity, using the method proposed by Zhang and collaborators and implemented in FSL-FAST v4.1 (Zhang et al., 2001). The unbiased T1-weighted images were then spatially transformed to match the 1 mm^3 MNI152 brain template (Fonov et al, 2009), using FSL-FLIRT (Jenkinson et al., 2002). This procedure included a two-step affine transformation, to minimize the alignment error of subcortical structures arising from spatial registration (Patenaude et al., 2011). First, a whole-brain linear transformation with 12 degrees of freedom was estimated for initial resampling to standard space. Next, a transformation was computed using a mask solely of the subcortical structures (bilateral thalamus, hippocampus, amygdala, lentiform and caudate nuclei), and then applied to the entire brain.

Additionally, in order to characterize the shape and volume of the thalamus, a Bayesian shape and appearance segmentation model (Patenaude et al., 2011) was applied to the preprocessed images (FSL-FIRST v5.0.0). In brief, to this end a three-

dimensional mesh was iteratively deformed to match the shape of the thalamus, while the voxel intensity was used to judge the goodness of fit. This novel and automatic procedure takes advantage of a training set comprising 336 manually labeled T1-weighted images and of the typical fixed topology of subcortical structures in order to define precisely the region of interest (ROI) corresponding to the thalamus. Since the three-dimensional meshes have a fixed number of vertices across subjects, FSL-FIRST estimates group differences not only for the overall volume of the ROI, but also for shape, corresponding respectively to indices of the global and local atrophy/hypertrophy. This latter analysis entails using a univariate test that estimates the mean distance of each vertex between groups (vertex analysis).

Individual thalamic ROIs generated by FSL-FIRST were carefully inspected to exclude the possibility of misclassification of thalamic voxels adjacent to the borders, although no manual correction proved to be necessary. Next, overall volumes of the left and right thalamus were measured for each subject (FSLSTATS) and imported in SPSS to investigate the expected differences in global volume between CB and SC. This hypothesis was tested ($p<0.05$) through a general linear model (GLM) including group, gender and scanner site in addition to age and overall brain volume as covariates.

To characterize the exact anatomical location for morphological changes of the thalamus due to congenital blindness, we performed a test on the coordinates of each vertex. A rigid alignment (global rotation and translation) was applied to the individual thalamic meshes, with the purpose of minimizing the sum of square error distance from the average thalamus shape. This procedure ensures the removal of error due to differences in pose of different subjects, while preserving the characteristics of the individual MRI acquisition. Just as for the overall thalamic

volume analysis, group, age, gender, MRI scanner location and total brain volume were included as factors in the GLM. A non-parametric permutation test with 10,000 iterations (Nichols and Holmes 2002) was applied to identify vertices showing significant ($p<0.05$) displacements between CB and SC, using the Threshold-Free Cluster Enhancement (TFCE) method to correct for multiple comparisons (Smith and Nichols, 2009).

Finally, to illustrate better regions of local alteration in the CB versus SC contrast, vertex analysis results were overlapped with the Oxford Thalamic Connectivity Probability Atlas (Behrens et al., 2003; Johansen-Berg et al., 2005). This atlas, which is included in the FSL 5.0 Software Library, provides a parcellation of the human thalamus to seven sub-regions based on thalamo-cortical connectivity, as distinguished in diffusion-weighted acquisitions in conjunction with probabilistic tractography analysis. Consequently, the anatomical locations demonstrating differences between groups were ultimately classified according to the cortical regions normally targeted by their projections: prefrontal, premotor, primary motor, somatosensory, posterior parietal, occipital and temporal cortices – for a precise definition of the boundaries of cortical regions please refer to Behrens et al., (2003). Thalamic nuclei equivalent to the tractography-defined subregions of the Oxford Thalamic Connectivity Probability Atlas are summarized in table 2, as proposed by Behrens et al., (2003). To summarize the results of the vertex-wise analysis and improve the readability of their relationship with the connectivity atlas, we built a flattened version of the thalamus. In brief, the 3-dimensional mesh was imported into Matlab and processed using the dpv2map tool, part of the Areal package (Winkler et al., 2012 - http://brainder.org/download/areal/). The obtained surface comprised both atlas values and vertex-wise statistics for group comparisons and was then imported

into Blender (http://www.blender.org/), cut in the dorsal part along the rostro-caudal axis of the thalamus and flattened, thereby correcting for geometrical distortions.

Table 2 about here

Therefore, for each of the Oxford Thalamic Connectivity subregions (projected onto the study-specific thalamus template as depicted in Figure 1), we extracted three '*atrophy scores*' for the CB versus SC group comparison: the average T-value, the maximum T-value and the proportion of statistically significant vertices. Then, we calculated the Z-values across subregions for each score and the specific portions of the thalamus were sorted accordingly from the most atrophic to the most preserved. Thus, the subregions were given a rank for each 'atrophy score' and subsequently we calculated a composite index based on the median rank of the three scores (see histograms in Figure 1). This may be considered a vertex-analysis based qualitative measure of how congenital loss of sight specifically affects thalamic subregions.

Moreover, to quantify local volume differences within thalamic sub-regions, we created a '*study-specific thalamus template*' by pooling the segmented structures from sighted and blind subjects. Within this 'averaged' thalamus, we estimated the volume of each subregion as the total voxel count weighted by (that is, multiplied by) the Oxford Thalamic Connectivity Probability Atlas values. Subsequently, at a single subject level, a displacement value (i.e., the output of the vertex analysis) was derived for each voxel as the geometric distance between the actual edge of each subject's thalamus and the edge of the *study-specific template*. In addition, for each subject, the

grand total of voxel displacements was weighted by connectivity values and was added to the volume of each specific subregion of the thalamic template.

The use of weighted (i.e., non-binary) ROIs takes into account the variability of the region across subjects and allows for an estimation of the atrophy, dealing with the degree of uncertainty on voxel identity. Therefore, volumetric changes between the groups were tested separately for each thalamic ROI by means of a GLM including gender, MRI location, age and overall brain volume as nuisance variables ($p<0.05$). Since the Oxford thalamic parcellation comprises seven subregions, a formal correction for multiple comparisons was carried out by means of the false discovery rate (FDR) procedure (Benjamini and Hochberg, 1995). In the last step, volume variations were also expressed as percentages (i.e., the average volume difference between groups, divided by the ROI volume of SC and multiplied by 100).

Volumetric Analysis of the Metathalamus

The metathalamus consists of the lateral and medial geniculate nuclei, respectively LGN and MGN; these are not included in the Oxford Thalamic Connectivity Probability Atlas, and their precise localization and volumetric measurement using T1 acquisitions remains a technical challenge (Gupta et al., 2009; Li et al., 2012). To overcome these problems, we adopted a ROI-based approach that combines an automatic segmentation method (Hernowo et al., 2011) with probabilistic maps registered to the MNI space (Bürgel et al., 1999; Rademacher et al., 2002; Eickhoff et al., 2005; Bürgel et al., 2006). Metathalamic nuclei are identified by partitioning the T1 brain image into six tissue classes (Hernowo et al., 2011), instead of the common segmentation of the three tissues: gray matter, white

matter and cerebrospinal fluid. The fifth tissue class of this fine grain parcellation, carried out using FSL-FAST v4.1 and based on voxel intensity (Zhang et al., 2001), accounts well for the boundary definition of diencephalic structures of present interest, i.e. the lateral and medial geniculate nuclei. The approach has been successfully used in a report that included normal controls and patients affected by primary open-angle glaucoma (Hernowo et al., 2011). In order to refine the bilateral LGN and MGN segmentation, four spherical ROIs of 10 mm diameter were used as an anatomical prior and were drawn at the center of gravity of the lateral and medial geniculate maps included in the Jülich cytoarchitectonic atlas (Eickhoff et al., 2005).

The maximum volume estimation of each spherical ROI was 524 mm^3, a value that according to previous post-mortem (Zvorykin, 1980; Winer, 1984; Andrews et al., 1997) and MRI studies (Korsholm et al., 2007; Hernowo et al., 2011; Li et al., 2012; Lee et al., 2014) is adequate to comprise the volume range for left and right lateral and medial geniculate nuclei. Moreover, the 10-mm diameter of the ROI comprises the 4 to 6 mm LGN height (Gupta et al., 2009; Dai et al., 2011) and accommodates the intersubject variability (Barnes et al., 2010). Once the lateral and medial geniculate nuclei were identified as outlined above, we computed the volume of the metathalamus following the tissue quantification guidelines (http://fsl.fmrib.ox.ac.uk/fsl/fslwiki/FAST). For each subject, the volumes of the LGN and MGN were estimated as the sum of the non-zero probability voxels lying inside the mask, multiplied by (i.e. limited to) the tissue probability map. As for the other ROI analyses, the statistically significant ($p<0.05$) group differences were estimated using a GLM adding age, gender, MRI site and overall brain volume as covariates of no interest.

Volumetric Analysis of the Superior and Inferior Colliculi

As for the volumetric analysis of the metathalamus, we used a semi-automatic ROI procedure to assess volumetric changes in the superior and inferior colliculi. As a first step, we manually aligned each subject's T1 image to the intercommissural plane (AC-PC line). We then adjusted brightness, contrast and color scale to facilitate the detection of these mesencephalic structures. Next, the borders of four ROIs (left and right superior and inferior colliculi) were manually drawn on sagittal, coronal and transverse sections following the definitions of the Duvernoy's atlas of the human brain stem and cerebellum (Naidich et al., 2009). The dorsolateral margins of the superior and inferior colliculi were carefully defined on coronal sections, at the level where they join the respective brachia. We defined the borders of the inferior colliculi on transverse and sagittal sections alongside the medullary lamina, excluding the thin band of the lateral lemniscus. Further, the medial border of the inferior colliculus was traced along the marginal fibers of the periaqueductal grey, while the upper boundary was delineated on a sagittal plane, exactly where the ellipsoidal body of the inferior colliculus joins the lower portion of the superior colliculus (similarly to Kang et al., 2008). The periaqueductal grey was taken to define medial and anterior borders of the superior colliculus, while the quadrigeminal cistern represented its posterior margin.

Once single subjects ROIs were defined, we extracted the absolute volume for each structure as the number of voxels within each mask multiplied by the parenchymal (GM + WM) tissue probability. Finally, we evaluated volumetric differences between blind and sighted participants for each structure (i.e., left and right superior and left and right inferior colliculus; $p<0.05$) by means of a GLM, using age, gender, MRI site and overall brain volume as nuisance variables.

Results

The overall brain parenchymal volume (GM + WM volume) was significantly decreased in congenitally blind subjects [F(1,46) = 5.334, p-value = 0.025], as compared to sighted individuals. This was confirmed by a whole brain voxel based morphometry (VBM) analysis showing patterns of white and grey matter atrophy similar to those available in the literature (see Supplementary Material for details).

Global and Local Volume Estimation of the Thalamus

Overall thalamic volume analysis demonstrated a significant reduction in both the left [F(1,46) = 7.599, p-value = 0.008] and right thalamus [F(1,46) = 7.931, p-value = 0.007] of blind participants. Specifically, volumes of the left thalamus (mean ± standard error) were 7651 ± 102 mm^3 for CB and 8037 ± 97 mm^3 for SC, whereas corresponding volumes of the right thalamus were 7462 ± 98 mm^3 and 7841 ± 93 mm^3, respectively. No gender-related or scanner site-specific effects were found.

Results of the vertex-wise (Fig.1) and ROI analyses (Fig.2) demonstrated a specific pattern of atrophy affecting the thalamus in the congenitally blind individuals. Loss of vision significantly altered regions of the left thalamus (Fig.1 and lower part of Fig.2B), which are connected with temporal [F(1,46) = 8.760, FDRc p-value = 0.023], occipital [F(1,46) = 8.742, FDRc p-value = 0.023] and prefrontal cortical areas [F(1,46) = 7.217, FDRc p-value = 0.035]. These regions had volume reductions of 9.76%, 8.51% and 4.54%, respectively. In addition, the left thalamic nuclei projecting to posterior parietal, somatosensory, premotor, and motor cortices showed no statistically significant atrophy (p>0.05). For the right thalamus, we

observed a 9.28% volume reduction (Fig.1 and lower part of Fig.2C) in nuclei projecting to temporal [F(1,46) = 8.561, FDRc p-value = 0.023], 5.53% to occipital [F(1,46) = 5.541, FDRc p-value = 0.048], 4.16% to premotor [F(1,46) = 5.430, FDRc p-value = 0.048] and 4.14% to prefrontal cortex [F(1,46) = 6.511, FDRc p-value = 0.039]. There were no significant volume changes in thalamic nuclei projecting to posterior parietal, motor and somatosensory cortex.

The heat-map plots located in the upper part of figure 2B and 2C depict the specific 'footprint' of local atrophy in the visually deprived thalami. Here, each thalamic sub-region is represented as a two-dimensional frequency distribution of voxels (color), that are characterized by the specificity of their projections (y-axis: connectivity scores extracted from the Oxford Thalamic Connectivity Probability Atlas) and by the magnitude of the atrophy in congenitally blind subjects (x-axis: T-values for CB<SC obtained from the vertex analysis). Indeed, it appears that voxels with higher connectivity values (i.e., with a specific attributable identity) represent the magnitude of local atrophy for the related thalamic sub-region. Thus, regions of the thalamus showing the most pronounced volumetric differences between groups (according to the bar charts in the lower part of panel 2B and 2C), have conspicuous clusters of specifically connected voxels that lie well above the statistical threshold (white dashed line: t(56) p=0.05), while thalamic nuclei that are not affected by congenital blindness demonstrate a considerable number of highly connected voxels lying below the threshold. On the other hand, for both impaired and preserved subregions, less specific voxels (that is, those with lower connectivity scores) have a broad range of atrophy scores, which is roughly homogeneous across thalamic nuclei. Therefore, local volume decrements found in thalamic sub-regions of the CB are not

merely driven by differences in the global thalamic volume, but originate from specific patterns of atrophy due to the absence of sight.

Figure 1 about here

Thus, according to our thalamic nuclei classification based on the thalamo-cortical connectivity proposed by Behrens and collaborators (2003), affected regions in the CB group included the inferior and medial pulvinar, the mediodorsal nucleus (MD), the ventral anterior nucleus (VA) and the anterior complex (AC). The ventral lateral (VLp), the anterior pulvinar, the ventral posteromedial (VPM) and the ventral posterolateral (VPL) nuclei did not show significant volumetric changes.

Figure 2 about here

Volumetric Analysis of the Metathalamus

In sighted controls the average volumes (mean ± standard error) for the left and right LGN were 135.2 ± 7.2 mm^3 and 133.4 ± 6.4 mm^3, while volumes for the medial geniculate nuclei were 95.7 ± 7.7 mm^3 (left MGN) and 92.4 ± 7.0 mm^3 (right MGN), respectively. Most importantly, a group comparison revealed volume reductions of 38.57% and 47.65%, respectively for the left [$F(1,46) = 27.180$, $p = 4\times10^{-6}$] and right [$F(1,46) = 50.426$, $p < 1\times10^{-6}$] LGN of blind individuals, while volumes of bilateral MGN did not differ between groups (Fig.3).

Noteworthy, volumetric measurements in our sighted controls were comparable to that reported in previous post-mortem studies, both for the lateral geniculate (Andrews et al., 1997) and the medial geniculate (Winer, 1984) nuclei.

Figure 3 about here

Volumetric Analysis of the Superior and Inferior Colliculi

Neither the superior, nor the inferior colliculi showed any statistically significant difference between the two groups (Fig. 4). Specifically, the average volumes of the superior colliculus of sighted controls (mean ± standard error) were 180.2 **±** 4.9 mm^3 (left) and 169.8 **±** 4.4 mm^3 (right), compared to 175.9 **±** 5.2 mm^3 (left) and 166.6 **±** 4.4 mm^3 (right) for congenitally blind subjects. Volumes of the left and right inferior colliculus were respectively 117.7 **±** 4.0 mm^3 and 110.6 **±** 3.9 mm^3 for SC, and 121.7 **±** 4.2 mm^3 and 108.2 **±** 4.1 mm^3 for CB.

Figure 4 about here

Discussion

In a multicenter MRI study sample of blind individuals contrasted with a matched sighted control group, we demonstrated that congenital loss of sight leads to an overall thalamic volume reduction. The lateral geniculate nucleus (i.e., the main visual thalamic relay) and the thalamic association nuclei projecting to the temporal (anterior complex, inferior and medial pulvinar), right premotor (ventral anterior), prefrontal (mediodorsal) and occipital (inferior pulvinar) cortical areas were affected. Interestingly, non-visual (auditory, motor and somatosensory) relay nuclei, such as the medial geniculate, posterior part of ventral lateral, ventral posteromedial and ventral posterolateral nuclei, were not reduced in volume. Of note, these nuclei did not show volume increases either, which is in contrast with what one might expect as previous studies showed a significant hypertrophy in both the somatosensory (Noppeney et al., 2005) and motor (Yu et al., 2007) pathways of blind subjects. Furthermore, in contrast to what one would expect based on results from animal studies, the superior colliculus in the congenitally blind individuals was preserved, indicating that the atrophy within the subcortical visual pathways is limited to diencephalic structures. The mesencephalic component of the auditory system (i.e., the inferior colliculus) was also within the normal range in congenitally blind subjects, thus suggesting that visual deprivation does not lead to a plasticity-induced compensatory hypertrophy in the subcortical auditory pathway.

The present findings expand the observation of volumetric and metabolic changes found in the neocortex of congenitally blind individuals (see Kupers and Ptito, 2011, 2014), by demonstrating that corresponding changes also occur in thalamic nuclei that project to their specific cortical target.

In general, sensory deprivation, especially at an early stage of development, results in a functional reorganization of the brain, which comes to rely more on the remaining sensory inputs. Consequently, cortical and subcortical visual structures in congenitally blind subjects undergo cross-modal plastic modifications that reshape their anatomical and physiological organization, making them more responsive to non-visual perceptual and cognitive tasks (Pietrini et al., 2004; Noppeney et al., 2005; Ricciardi et al., 2009; Kupers and Ptito, 2011, 2014; Tomaiuolo et al., 2014).

The present data demonstrate that local atrophy of the primary visual relay nuclei, and also of the association nuclei in CB individuals, constitutes a specific pattern rather than some non-specific global reduction of the thalamus deprived of its normal visual input. In order to better define the 'footprint' of local volumetric alterations, the changes revealed by the vertex-wise analysis were assigned to still smaller sub-regions, parcellated according to their thalamo-cortical connections, as defined in the Oxford Atlas (Fig.2). Notably, although each division of the thalamus comprises both 'aspecific' (those with lower connectivity scores) and highly specific (those with higher cortical connectivity rates) voxels, it is the latter group that determines the local volume reduction in the CB. Hence, thalamic voxels assigned less cortical connectivity have a wider range of "atrophy" scores, homogeneous across thalamic nuclei. Thus, within each thalamic sub-region, those clusters with a distinct 'identity' in terms of their normal connectivity were preserved or affected by congenital loss of sight in a manner consistent with their functional role, and the predictability of their cortical projections. Again, this finding supports our hypothesis that sub-regional volume decrements in CB are not simply a consequence of a decline in the global

thalamic volume, but arise from a specific pattern of atrophy due to the congenital absence of sight.

Two distinct mechanisms might be put forward to explain the thalamic volume loss in congenitally blind individuals, namely (1) changes in reciprocal thalamo-cortical connections and (2) changes in the intrinsic connectivity between thalamic relay and association nuclei. We found volume loss in both primary visual and association thalamic nuclei, including the pulvinar and the mediodorsal nuclei. The association nuclei integrate multiple sensory and motor inputs/outputs, and have a pivotal role in regulating the neural activity of associative cortical areas through a complex network of reciprocal connections (Hendelman, 2005). We suggest that the lack of visual input triggers a cascade of atrophic or developmental changes, arising first in the LGN, extending to the optic radiations (Ptito et al., 2008; our VBM results), and ultimately further to striate and extra-striate cortices. At the same time, default cortico-cortical connectivity of these normally visual cortical areas with parietal, frontal and temporal cortical areas are also reduced (Liu et al., 2007), consequently attenuating the feedback connections between parietal, frontal and temporal cortices with their recipient thalamic nuclei. In this regard, we find it noteworthy that a recent resting state functional connectivity study in the sighted showed that specific thalamic structures exhibit BOLD signal fluctuations in phase with those of their connected cortical regions, underscoring the importance of the cortico-thalamic feedback and feed-forward projections (Zhang et al., 2008). On the other hand, the results of task-related functional connectivity analyses, mainly involving perceptual tasks, seem to suggest that cross-modal plastic changes in the CB reflect alterations more in cortico-cortical rather than thalamo-cortical

connections (Klinge et al., 2010; Collignon et al., 2013; Leo et al., 2012; Kupers and Ptito, 2014; but see also Kahn and Krubitzer, 2002; Desgent and Ptito, 2012).

Alternatively, volume reductions may reflect reshaping of the thalamic maps, a process suggested by Kahn & Krubitzer (2002). According to this view, rewiring of the intrinsic thalamic connections takes place in blindness, leading to a "colonization" of normally visual thalamic nuclei by other nuclei receiving non-visual input. This hypothesis is to a certain extent supported by observations in animal studies. For instance, Heil and colleagues (1991) found that both the visual cortex and the LGN of the blind mole rat receive auditory inputs, while Chabot and collaborators (2007) reported auditory-evoked electrophysiological activity in the LGN of anophthalmic mice. Thus, in the event of the lack of a distinct sensory modality, such as the visual one, the developmental differentiation program may attract other sensory inputs to continue the thalamic maturation (recently reviewed in Ricciardi et al., 2013). Nonetheless, this 'hard-rewiring' hypothesis and the modifications occurring in the cortico-thalamic feedback connections may equally contribute to and reciprocally interact in the reshaping of the thalamus in visually deprived individuals.

Moreover, the mere fact that all retinal inputs are absent since birth should theoretically lead to a degeneration of the dorsal lateral geniculate nucleus (dLGN), as shown in animal models of neonatal enucleation (see Desgent and Ptito, 2012, for review). Indeed, in bilaterally enucleated animals, the dLGN is reduced by approximately one half (Heumann and Rabinowicz, 1980), although its remaining neurons still project via the optic radiations to the visual cortex. In accordance with that study, and with a previous one conducted on CB humans (Ptito et al., 2008), we now report that early loss of sight leads to a dramatic volume reduction in bilateral

LGN and in their striate projections (see Supplementary results). We believe that the remaining LGN stays functional thanks to the cortico-thalamic inputs it receives from the striate cortex, which has adopted non-visual functions. Indeed, the visual cortex of CB receives two types of non-visual inputs, arising either through the optic radiations from a dLGN which has been "colonized" by VPL or MGB, and as ectopic projections from mesencephalic structures, such as the inferior colliculus, or through altered cortico-cortical projections back to the dLGN (Ptito and Kupers 2005; Ptito et al., 2005; Kupers et al., 2006; Ioannides et al., 2013).

As far as the superior colliculus is concerned, volumes obtained in the sighted controls using our procedure are in line with those reported in previous studies (Kang et al., 2008; Sabanciogullari et al., 2013) and with those we obtained when using an alternative independent volumetric evaluation on the MNI152 Standard Symmetric Template (see Supplementary Materials). Two factors may explain the lack of volume reduction in the superior colliculus of congenitally blind subjects: (a) a significant proportion of its neurons, located in the deep layers, responds to multisensory inputs (Sparks and Hartswitch-Young, 1989) and (b) the number of retinotectal projections, that target only the superficial layers of the colliculus (Tiao and Blackmore, 1976; Wallace et al., 1996; Katyal et al., 2010), decreases along with the phylogenetical evolution of the geniculostriate system (Schiller, 1977; White and Munoz, 2011). In conclusion, unlike the lateral geniculate nucleus, the human superior colliculus cannot be regarded as a merely visual structure, and this may explain the lack of significant effects following perinatal visual deprivation.

In summary, using structural MRI in a multicenter study sample of congenitally blind humans, we show that absence of sight reduces by half the volume of the primary visual relay (LGN), with additional significant, though smaller, reductions in

non-visual association thalamic nuclei. Importantly, the volumes of the remaining sensory relay nuclei, as well as the superior colliculus, were not affected. We propose a model whereby, because of the absence of vision since birth, the visual relay and association nuclei of the thalamus undergo a massive re-organization of their circuitry through abnormal intra-thalamic connectivity, and the retention of cortico-thalamic projections from the re-organized primary visual cortex (which has assumed non-visual functions), as well as from other cortical regions.

Figure Legends

Fig.1 Vertex-wise analysis in congenitally blind as compared to sighted control subjects. The flattened version of the left and right study-specific thalamus template is shown in the upper part of the panel and subregions of the Oxford Thalamic Connectivity Probability atlas are projected onto the surface. Vertices projecting to prefrontal (PFC) cortical areas are depicted in cyan, premotor cortex (PMC) in purple, motor cortex (MC) in red, somatosensory cortex (SSC) in green, posterior parietal cortex (PPC) in dark-blue, temporal cortex (TC) in yellow and occipital cortex (OC) in orange. Each subregion is also individually represented to improve the readability of vertex-wise statistics (t-values for group comparison). In the lower part of the panel, the histogram represents the Z-scores across subregions for the average T-value, the maximum T-value and the atrophy proportion of vertices. Thalamic regions are sorted according to the median rank of the three 'atrophy scores', from the most preserved to the most atrophic. As shown, congenital loss of sight affects the thalamic subregions to different extents. Interestingly, none of the thalamic areas was significantly larger in blind participants.

Fig.2 Results of the ROI analysis. Both the global and local volumes of the thalamus were compared between groups. Bar charts in panel 2A show the statistically significant overall volume reduction in the left and right thalamus of CB. The axial brain slice in 2A represents the 'color-code' used to define portions of the thalamus according to the Oxford Thalamic Connectivity Probability Atlas (Behrens

et al., 2003; Johansen-Berg et al., 2005). The figure also shows local volume loss for the left (2B) and right (2C) sub-regions of the thalamus projecting to SSC (green), PPC (blue), OC (orange), TC (yellow) PFC (cyan), PMC (purple) and MC (red). The bar charts located in the lower part of these panels reveal thalamic subregions showing a statistically significant volume reduction due to congenital blindness. In agreement with this, the upper part of the panels shows that regions affected by lack of vision have a noticeable proportion (hotter colors) of highly specific voxels (with higher scores of connectivity), demonstrating larger spatial displacement values between groups (higher T-values for CB<SC). The white dashed line represents t(56) p=0.05, just for readability purpose

Fig.3 Results for the volumetric analysis of lateral (LGN) and medial (MGN) geniculate nucleus. The upper part of the panel depicts the LGN and MGN segmentation in two representative subjects. The histogram, located in the lower part of the figure, reveals a significant difference ($p<0.05$) between CB and SC in the bilateral LGN but not in the MGN

Fig.4 Volumetric analysis of the superior (SUPc) and inferior (INFc) colliculus. The upper part of the panel illustrates the delineation of these structures for the MNI template (white line and black arrow) and for two representative subjects (black arrows), CB25 and SC21. No significant differences between CB and SC were found for either the superior or inferior colliculus (bar chart, lower part).

Acknowledgments

LC would like to thank Dr. Francesco Tomaiuolo and Dr. Ludwig Barbaro for the helpful comments and suggestions provided. This work was supported by grants from the Italian Ministero dell'Istruzione, dell'Università e della Ricerca (PP, ER, LC, GH), the Lundbeck foundation (RK), the Danish Medical Research Council (MP), and the Harland Sanders Chair in Visual Science (Canada). The authors note professional manuscript proofreading by Inglewood Biomedical Editing.

Conflict of Interest

None of the authors has any potential conflict of interest related to this manuscript.

References

Andrews TJ, Halpern SD, Purves D (1997) Correlated size variations in human visual cortex, lateral geniculate nucleus, and optic tract. The Journal of neuroscience : the official journal of the Society for Neuroscience 17:2859-2868

Ashburner J (2007) A fast diffeomorphic image registration algorithm. NeuroImage 38:95-113 doi:10.1016/j.neuroimage.2007.07.007

Ashburner J, Friston KJ (2005) Unified segmentation. NeuroImage 26:839-851 doi:10.1016/j.neuroimage.2005.02.018

Barnes GR, Li X, Thompson B, Singh KD, Dumoulin SO, Hess RF (2010) Decreased gray matter concentration in the lateral geniculate nuclei in human amblyopes. Investigative ophthalmology & visual science 51:1432-1438 doi:10.1167/iovs.09-3931

Bavelier D, Neville HJ (2002) Cross-modal plasticity: where and how?. Nature reviews Neuroscience 3:443-452 doi:10.1038/nrn848

Behrens TE et al. (2003) Non-invasive mapping of connections between human thalamus and cortex using diffusion imaging. Nature neuroscience 6:750-757 doi:10.1038/nn1075

Benjamini Y, Hochberg Y (1995) Controlling the false discovery rate: a practical and powerful approach to multiple testing. J Roy Statist Soc B 57:289-300

Berardi N, Pizzorusso T, Maffei L (2000) Critical periods during sensory development. Current opinion in neurobiology 10:138-145

Bonino D et al. (2008) Tactile spatial working memory activates the dorsal extrastriate cortical pathway in congenitally blind individuals. Archives italiennes de biologie 146:133-146

Bridge H, Cowey A, Ragge N, Watkins K (2009) Imaging studies in congenital anophthalmia reveal preservation of brain architecture in 'visual' cortex. Brain : a journal of neurology 132:3467-3480 doi:10.1093/brain/awp279

Burgel U, Amunts K, Hoemke L, Mohlberg H, Gilsbach JM, Zilles K (2006) White matter fiber tracts of the human brain: three-dimensional mapping at microscopic resolution, topography and intersubject variability. NeuroImage 29:1092-1105 doi:10.1016/j.neuroimage.2005.08.040

Burgel U, Schormann T, Schleicher A, Zilles K (1999) Mapping of histologically identified long fiber tracts in human cerebral hemispheres to the MRI volume of a reference brain: position and spatial variability of the optic radiation. NeuroImage 10:489-499 doi:10.1006/nimg.1999.0497

Burnett LR, Stein BE, Chaponis D, Wallace MT (2004) Superior colliculus lesions preferentially disrupt multisensory orientation Neuroscience 124:535-547 doi:10.1016/j.neuroscience.2003.12.026

Cappe C, Morel A, Barone P, Rouiller EM (2009) The thalamocortical projection systems in primate: an anatomical support for multisensory and sensorimotor interplay. Cerebral cortex 19:2025-2037 doi:10.1093/cercor/bhn228

Cattaneo Z, Vecchi T, Cornoldi C, Mammarella I, Bonino D, Ricciardi E, Pietrini P (2008) Imagery and spatial processes in blindness and visual impairment. Neuroscience and biobehavioral reviews 32:1346-1360 doi:10.1016/j.neubiorev.2008.05.002

Chabot N, Robert S, Tremblay R, Miceli D, Boire D, Bronchti G (2007) Audition differently activates the visual system in neonatally enucleated mice compared with anophthalmic mutants. The European journal of

neuroscience 26:2334-2348 doi:10.1111/j.1460-9568.2007.05854.x

Chebat DR, Chen JK, Schneider F, Ptito A, Kupers R, Ptito M (2007) Alterations in right posterior hippocampus in early blind individuals. Neuroreport 18:329-333 doi:10.1097/WNR.0b013e32802b70f8

Chen Z, Wang J, Lin F, Dai H, Mu K, Zhang H (2013) Correlation between lateral geniculate nucleus atrophy and damage to the optic disc in glaucoma. Journal of neuroradiology Journal de neuroradiologie 40:281-287 doi:10.1016/j.neurad.2012.10.004

Collignon O, Dormal G, Albouy G, Vandewalle G, Voss P, Phillips C, Lepore F (2013) Impact of blindness onset on the functional organization and the connectivity of the occipital cortex. Brain : a journal of neurology 136:2769-2783 doi:10.1093/brain/awt176

Crish SD, Dengler-Crish CM, Catania KC (2006) Central visual system of the naked mole-rat (Heterocephalus glaber) The anatomical record Part A, Discoveries in molecular, cellular, and evolutionary biology 288:205-212 doi:10.1002/ar.a.20288

Cullen MJ, Kaiserman-Abramof IR (1976) Cytological organization of the dorsal lateral geniculate nuclei in mutant anophthalmic and postnatally enucleated mice. Journal of neurocytology 5:407-424

Dai H et al. (2011) Assessment of lateral geniculate nucleus atrophy with 3T MR imaging and correlation with clinical stage of glaucoma. AJNR American journal of neuroradiology 32:1347-1353 doi:10.3174/ajnr.A2486

Desgent S, Ptito M (2012) Cortical GABAergic interneurons in cross-modal plasticity following early blindness. Neural plasticity 2012:590725 doi:10.1155/2012/590725

DuBois RM, Cohen MS (2000) Spatiotopic organization in human superior colliculus observed with fMRI NeuroImage 12:63-70 doi:10.1006/nimg.2000.0590

Ehrsson HH (2007) The experimental induction of out-of-body experiences. Science 317:1048 doi:10.1126/science.1142175

Eickhoff SB, Stephan KE, Mohlberg H, Grefkes C, Fink GR, Amunts K, Zilles K (2005) A new SPM toolbox for combining probabilistic cytoarchitectonic maps and functional imaging data. NeuroImage 25:1325-1335 doi:10.1016/j.neuroimage.2004.12.034

Felleman DJ, Van Essen DC (1991) Distributed hierarchical processing in the primate cerebral cortex. Cerebral cortex 1:1-47

Fonov V, Evans AC, Botteron K, Almli CR, McKinstry RC, Collins DL, Brain Development Cooperative G (2011) Unbiased average age-appropriate atlases for pediatric studies. NeuroImage 54:313-327 doi:10.1016/j.neuroimage.2010.07.033

Fortin M et al. (2008) Wayfinding in the blind: larger hippocampal volume and supranormal spatial navigation. Brain : a journal of neurology 131:2995-3005 doi:10.1093/brain/awn250

Frost DO, Boire D, Gingras G, Ptito M (2000) Surgically created neural pathways mediate visual pattern discrimination. Proceedings of the National Academy of Sciences of the United States of America 97:11068-11073 doi:10.1073/pnas.190179997

Ghazanfar AA, Schroeder CE (2006) Is neocortex essentially multisensory?. Trends in cognitive sciences 10:278-285 doi:10.1016/j.tics.2006.04.008

Good CD, Johnsrude IS, Ashburner J, Henson RN, Friston KJ, Frackowiak RS

(2001) A voxel-based morphometric study of ageing in 465 normal adult human brains. NeuroImage 14:21-36 doi:10.1006/nimg.2001.0786

Gupta N, Greenberg G, de Tilly LN, Gray B, Polemidiotis M, Yucel YH (2009) Atrophy of the lateral geniculate nucleus in human glaucoma detected by magnetic resonance imaging. The British journal of ophthalmology 93:56-60 doi:10.1136/bjo.2008.138172

Headon MP, Powell TP (1973) Cellular changes in the lateral geniculate nucleus of infant monkeys after suture of the eyelids. Journal of anatomy 116:135-145

Heil P, Bronchti G, Wollberg Z, Scheich H (1991) Invasion of visual cortex by the auditory system in the naturally blind mole rat. Neuroreport 2:735-738

Hendelman WJ (2005) Atlas of functional neuroanatomy. 2nd ed. CRC Press, Boca Raton (FL)

Hernowo AT, Boucard CC, Jansonius NM, Hooymans JM, Cornelissen FW (2011) Automated morphometry of the visual pathway in primary open-angle glaucoma. Investigative ophthalmology & visual science 52:2758-2766 doi:10.1167/iovs.10-5682

Heumann D, Rabinowicz T (1980) Postnatal development of the dorsal lateral geniculate nucleus in the normal and enucleated albino mouse. Experimental brain research 38:75-85

Hilbig H, Bidmon HJ, Zilles K, Busecke K (1999) Neuronal and glial structures of the superficial layers of the human superior colliculus Anatomy and embryology 200:103-115

Iglesias JE, Liu CY, Thompson PM, Tu Z (2011) Robust brain extraction across datasets and comparison with publicly available methods. IEEE

transactions on medical imaging 30:1617-1634 doi:10.1109/TMI.2011.2138152

Ioannides AA, Liu L, Poghosyan V, Saridis GA, Gjedde A, Ptito M, Kupers R (2013) MEG reveals a fast pathway from somatosensory cortex to occipital areas via posterior parietal cortex in a blind subject. Frontiers in human neuroscience 7:429 doi:10.3389/fnhum.2013.00429

Jenkinson M, Bannister P, Brady M, Smith S (2002) Improved optimization for the robust and accurate linear registration and motion correction of brain images. NeuroImage 17:825-841

Jenkinson M, Beckmann CF, Behrens TE, Woolrich MW, Smith SM (2012) Fsl. NeuroImage 62:782-790 doi:10.1016/j.neuroimage.2011.09.015

Jiang J et al. (2009) Thick visual cortex in the early blind. The Journal of neuroscience : the official journal of the Society for Neuroscience 29:2205-2211 doi:10.1523/JNEUROSCI.5451-08.2009

Johansen-Berg H, Behrens TE, Sillery E, Ciccarelli O, Thompson AJ, Smith SM, Matthews PM (2005) Functional-anatomical validation and individual variation of diffusion tractography-based segmentation of the human thalamus. Cerebral cortex 15:31-39 doi:10.1093/cercor/bhh105

Kahn DM, Krubitzer L (2002) Retinofugal projections in the short-tailed opossum (Monodelphis domestica). The Journal of comparative neurology 447:114-127 doi:10.1002/cne.10206

Kang DH, Kwon KW, Gu BM, Choi JS, Jang JH, Kwon JS (2008) Structural abnormalities of the right inferior colliculus in schizophrenia Psychiatry research 164:160-165 doi:10.1016/j.pscychresns.2007.12.023

Karlen SJ, Kahn DM, Krubitzer L (2006) Early blindness results in abnormal

corticocortical and thalamocortical connections. Neuroscience 142:843-858 doi:10.1016/j.neuroscience.2006.06.055

Karlen SJ, Krubitzer L (2009) Effects of bilateral enucleation on the size of visual and nonvisual areas of the brain. Cerebral cortex 19:1360-1371 doi:10.1093/cercor/bhn176

Katyal S, Zughni S, Greene C, Ress D (2010) Topography of covert visual attention in human superior colliculus Journal of neurophysiology 104:3074-3083 doi:10.1152/jn.00283.2010

Klinge C, Eippert F, Roder B, Buchel C (2010) Corticocortical connections mediate primary visual cortex responses to auditory stimulation in the blind. The Journal of neuroscience : the official journal of the Society for Neuroscience 30:12798-12805 doi:10.1523/JNEUROSCI.2384-10.2010

Korsholm K, Madsen KH, Frederiksen JL, Skimminge A, Lund TE (2007) Recovery from optic neuritis: an ROI-based analysis of LGN and visual cortical areas. Brain : a journal of neurology 130:1244-1253 doi:10.1093/brain/awm045

Krebs RM et al. (2010) High-field FMRI reveals brain activation patterns underlying saccade execution in the human superior colliculus PloS one 5:e8691 doi:10.1371/journal.pone.0008691

Kupers R, Beaulieu-Lefebvre M, Schneider FC, Kassuba T, Paulson OB, Siebner HR, Ptito M (2011) Neural correlates of olfactory processing in congenital blindness. Neuropsychologia 49:2037-2044 doi:10.1016/j.neuropsychologia.2011.03.033

Kupers R, Fumal A, de Noordhout AM, Gjedde A, Schoenen J, Ptito M (2006) Transcranial magnetic stimulation of the visual cortex induces

somatotopically organized qualia in blind subjects. Proceedings of the National Academy of Sciences of the United States of America 103:13256-13260 doi:10.1073/pnas.0602925103

Kupers R, Ptito M (2011) Insights from darkness: what the study of blindness has taught us about brain structure and function. Progress in brain research 192:17-31 doi:10.1016/B978-0-444-53355-5.00002-6

Kupers R, Ptito M (2014) Compensatory plasticity and cross-modal reorganization following early visual deprivation. Neuroscience and biobehavioral reviews 41:36-52 doi:10.1016/j.neubiorev.2013.08.001

Lee JY et al. (2014) An investigation of lateral geniculate nucleus volume in patients with primary open-angle glaucoma using 7 tesla magnetic resonance imaging. Investigative ophthalmology & visual science 55:3468-3476 doi:10.1167/iovs.14-13902

Leh SE, Johansen-Berg H, Ptito A (2006) Unconscious vision: new insights into the neuronal correlate of blindsight using diffusion tractography Brain : a journal of neurology 129:1822-1832 doi:10.1093/brain/awl111

Leh SE, Ptito A, Schonwiesner M, Chakravarty MM, Mullen KT (2010) Blindsight mediated by an S-cone-independent collicular pathway: an fMRI study in hemispherectomized subjects Journal of cognitive neuroscience 22:670-682 doi:10.1162/jocn.2009.21217

Leo A, Bernardi G, Handjaras G, Bonino D, Ricciardi E, Pietrini P (2012) Increased BOLD variability in the parietal cortex and enhanced parieto-occipital connectivity during tactile perception in congenitally blind individuals. Neural plasticity 2012:720278 doi:10.1155/2012/720278

Lepore N et al. (2009) Pattern of hippocampal shape and volume differences in

blind subjects. NeuroImage 46:949-957 doi:10.1016/j.neuroimage.2009.01.071

Lepore N et al. (2010) Brain structure changes visualized in early- and late-onset blind subjects. NeuroImage 49:134-140 doi:10.1016/j.neuroimage.2009.07.048

Li M et al. (2012) Quantification of the human lateral geniculate nucleus in vivo using MR imaging based on morphometry: volume loss with age. AJNR American journal of neuroradiology 33:915-921 doi:10.3174/ajnr.A2884

Limbrick-Oldfield EH, Brooks JC, Wise RJ, Padormo F, Hajnal JV, Beckmann CF, Ungless MA (2012) Identification and characterisation of midbrain nuclei using optimised functional magnetic resonance imaging NeuroImage 59:1230-1238 doi:10.1016/j.neuroimage.2011.08.016

Liu Y et al. (2007) Whole brain functional connectivity in the early blind. Brain : a journal of neurology 130:2085-2096 doi:10.1093/brain/awm121

Lund RD, Lund JS (1971) Synaptic adjustment after deafferentation of the superior colliculus of the rat Science 171:804-807

Masucci EF, Borts FT, Perl SM, Wener L, Schwankhaus J, Kurtzke JF (1995) MR vs CT in progressive supranuclear palsy Computerized medical imaging and graphics : the official journal of the Computerized Medical Imaging Society 19:361-368

May PJ (2006) The mammalian superior colliculus: laminar structure and connections Progress in brain research 151:321-378 doi:10.1016/S0079-6123(05)51011-2

Merabet LB, Pascual-Leone A (2010) Neural reorganization following sensory loss: the opportunity of change. Nature reviews Neuroscience 11:44-52

doi:10.1038/nrn2758

Naidich TP, Duvernoy HM, Delman BN, Sorensen AG, Kollias SS, Haacke EM (2009) Duvernoy's Atlas of the Human Brain Stem and Cerebellum. Springer, Wien

Nichols TE, Holmes AP (2002) Nonparametric permutation tests for functional neuroimaging: a primer with examples. Human brain mapping 15:1-25

Noppeney U (2007) The effects of visual deprivation on functional and structural organization of the human brain. Neuroscience and biobehavioral reviews 31:1169-1180 doi:10.1016/j.neubiorev.2007.04.012

Noppeney U, Friston KJ, Ashburner J, Frackowiak R, Price CJ (2005) Early visual deprivation induces structural plasticity in gray and white matter. Current biology : CB 15:R488-490 doi:10.1016/j.cub.2005.06.053

Pan WJ, Wu G, Li CX, Lin F, Sun J, Lei H (2007) Progressive atrophy in the optic pathway and visual cortex of early blind Chinese adults: A voxel-based morphometry magnetic resonance imaging study. NeuroImage 37:212-220 doi:10.1016/j.neuroimage.2007.05.014

Park HJ, Lee JD, Kim EY, Park B, Oh MK, Lee S, Kim JJ (2009) Morphological alterations in the congenital blind based on the analysis of cortical thickness and surface area. NeuroImage 47:98-106 doi:10.1016/j.neuroimage.2009.03.076

Patenaude B, Smith SM, Kennedy DN, Jenkinson M (2011) A Bayesian model of shape and appearance for subcortical brain segmentation. NeuroImage 56:907-922 doi:10.1016/j.neuroimage.2011.02.046

Pavani F, Spence C, Driver J (2000) Visual capture of touch: out-of-the-body experiences with rubber gloves. Psychological science 11:353-359

Pietrini P et al. (2004) Beyond sensory images: Object-based representation in the human ventral pathway. Proceedings of the National Academy of Sciences of the United States of America 101:5658-5663 doi:10.1073/pnas.0400707101

Ptito M, Desgent S (2006) Sensory Input–Based Adaptation and Brain Architecture. In: Baltes PB, Reuter-Lorenz PA, Rosler F, (ed) Lifespan Development and the Brain. Cambridge University Press, Cambridge, pp 111-133.

Ptito M, Kupers R (2005) Cross-modal plasticity in early blindness. Journal of integrative neuroscience 4:479-488

Ptito M, Moesgaard SM, Gjedde A, Kupers R (2005) Cross-modal plasticity revealed by electrotactile stimulation of the tongue in the congenitally blind. Brain : a journal of neurology 128:606-614 doi:10.1093/brain/awh380

Ptito M, Schneider FC, Paulson OB, Kupers R (2008) Alterations of the visual pathways in congenital blindness. Experimental brain research 187:41-49 doi:10.1007/s00221-008-1273-4

Qin W, Xuan Y, Liu Y, Jiang T, Yu C (2014) Functional Connectivity Density in Congenitally and Late Blind Subjects. Cerebral cortex doi:10.1093/cercor/bhu051

Rademacher J, Burgel U, Zilles K (2002) Stereotaxic localization, intersubject variability, and interhemispheric differences of the human auditory thalamocortical system. NeuroImage 17:142-160

Rhoades RW (1980) Effects of neonatal enucleation on the functional organization of the superior colliculus in the golden hamster The Journal of physiology

301:383-399

Ricciardi E, Bonino D, Pellegrini S, Pietrini P (2014) Mind the blind brain to understand the sighted one! Is there a supramodal cortical functional architecture?. Neuroscience and biobehavioral reviews 41:64-77 doi:10.1016/j.neubiorev.2013.10.006

Ricciardi E et al. (2009) Do we really need vision? How blind people "see" the actions of others. The Journal of neuroscience : the official journal of the Society for Neuroscience 29:9719-9724 doi:10.1523/JNEUROSCI.0274-09.2009

Ricciardi E, Handjaras G, Bonino D, Vecchi T, Fadiga L, Pietrini P (2013) Beyond motor scheme: a supramodal distributed representation in the action-observation network. PloS one 8:e58632 doi:10.1371/journal.pone.0058632

Ricciardi E, Pietrini P (2011) New light from the dark: what blindness can teach us about brain function. Current opinion in neurology 24:357-363 doi:10.1097/WCO.0b013e328348bdbf

Ricciardi E et al. (2007) The effect of visual experience on the development of functional architecture in hMT+. Cerebral cortex 17:2933-2939 doi:10.1093/cercor/bhm018

Sabanciogullari V, Salk I, Balaban H, Oztoprak I, Kelkit S, Cimen M (2013) Magnetic resonance imaging mesencephalic tectum dimensions according to age and gender Neurosciences 18:33-39

Sakakura H, Iwama K (1967) Effects of bilateral eye enucleation upon single unit activity of the lateral geniculate body in free behaving cats. Brain research 6:667-678

Schiller PH (1977) The effect of superior colliculus ablation on saccades elicted by cortical stimulation Brain research 122:154-156

Schmid B, Schindelin J, Cardona A, Longair M, Heisenberg M (2010) A high-level 3D visualization API for Java and ImageJ. BMC bioinformatics 11:274 doi:10.1186/1471-2105-11-274

Schneider KA, Kastner S (2009) Effects of sustained spatial attention in the human lateral geniculate nucleus and superior colliculus The Journal of neuroscience : the official journal of the Society for Neuroscience 29:1784-1795 doi:10.1523/JNEUROSCI.4452-08.2009

Sharma J, Angelucci A, Sur M (2000) Induction of visual orientation modules in auditory cortex. Nature 404:841-847 doi:10.1038/35009043

Sherman JL, Citrin CM, Barkovich AJ, Bowen BJ (1987) MR imaging of the mesencephalic tectum: normal and pathologic variations AJNR American journal of neuroradiology 8:59-64

Shimony JS, Burton H, Epstein AA, McLaren DG, Sun SW, Snyder AZ (2006) Diffusion tensor imaging reveals white matter reorganization in early blind humans. Cerebral cortex 16:1653-1661 doi:10.1093/cercor/bhj102

Shu N, Liu Y, Li J, Li Y, Yu C, Jiang T (2009) Altered anatomical network in early blindness revealed by diffusion tensor tractography. PloS one 4:e7228 doi:10.1371/journal.pone.0007228

Smith SA, Bedi KS (1997) Unilateral eye enucleation in adult rats causes neuronal loss in the contralateral superior colliculus Journal of anatomy 190 (Pt 4):481-490

Smith SM et al. (2004) Advances in functional and structural MR image analysis and implementation as FSL. NeuroImage 23 Suppl 1:S208-219

doi:10.1016/j.neuroimage.2004.07.051

Smith SM, Nichols TE (2009) Threshold-free cluster enhancement: addressing problems of smoothing, threshold dependence and localisation in cluster inference. NeuroImage 44:83-98 doi:10.1016/j.neuroimage.2008.03.061

Sparks DL, Hartwich-Young R (1989) The deep layers of the superior colliculus Reviews of oculomotor research 3:213-255

Sur M, Garraghty PE, Roe AW (1988) Experimentally induced visual projections into auditory thalamus and cortex. Science 242:1437-1441

Sylvester R, Josephs O, Driver J, Rees G (2007) Visual FMRI responses in human superior colliculus show a temporal-nasal asymmetry that is absent in lateral geniculate and visual cortex Journal of neurophysiology 97:1495-1502 doi:10.1152/jn.00835.2006

Theoret H, Boire D, Herbin M, Ptito M (2001) Anatomical sparing in the superior colliculus of hemispherectomized monkeys Brain research 894:274-280

Tiao YC, Blakemore C (1976) Functional organization in the superior colliculus of the golden hamster The Journal of comparative neurology 168:483-503 doi:10.1002/cne.901680404

Tomaiuolo F et al. (2014) Morphometric changes of the corpus callosum in congenital blindness PloS one 9:e107871 doi:10.1371/journal.pone.0107871

Trampel R, Ott DV, Turner R (2011) Do the congenitally blind have a stria of Gennari? First intracortical insights in vivo. Cerebral cortex 21:2075-2081 doi:10.1093/cercor/bhq282

Van Essen DC, Drury HA, Dickson J, Harwell J, Hanlon D, Anderson CH (2001) An integrated software suite for surface-based analyses of cerebral cortex.

Journal of the American Medical Informatics Association : JAMIA 8:443-459

von Melchner L, Pallas SL, Sur M (2000) Visual behaviour mediated by retinal projections directed to the auditory pathway. Nature 404:871-876 doi:10.1038/35009102

Wallace MT, Stein BE (1994) Cross-modal synthesis in the midbrain depends on input from cortex Journal of neurophysiology 71:429-432

Wallace MT, Wilkinson LK, Stein BE (1996) Representation and integration of multiple sensory inputs in primate superior colliculus Journal of neurophysiology 76:1246-1266

Wang D, Qin W, Liu Y, Zhang Y, Jiang T, Yu C (2014) Altered resting-state network connectivity in congenital blind. Human brain mapping 35:2573-2581 doi:10.1002/hbm.22350

Warmuth-Metz M, Naumann M, Csoti I, Solymosi L (2001) Measurement of the midbrain diameter on routine magnetic resonance imaging: a simple and accurate method of differentiating between Parkinson disease and progressive supranuclear palsy Archives of neurology 58:1076-1079

White BJ, Munoz DP (2011) The superior colliculus. In: Liversedge S, Gilchrist I, Everling S (ed) Oxford handbook of eye movements, 1st edn. Oxford University Press, New York, pp 195–213

Winer JA (1984) The human medial geniculate body. Hearing research 15:225-247

Winkler AM et al. (2012) Measuring and comparing brain cortical surface area and other areal quantities NeuroImage 61:1428-1443 doi:10.1016/j.neuroimage.2012.03.026

Yu C, Shu N, Li J, Qin W, Jiang T, Li K (2007) Plasticity of the corticospinal tract in early blindness revealed by quantitative analysis of fractional anisotropy based on diffusion tensor tractography. NeuroImage 36:411-417 doi:10.1016/j.neuroimage.2007.03.003

Zhang D, Snyder AZ, Fox MD, Sansbury MW, Shimony JS, Raichle ME (2008) Intrinsic functional relations between human cerebral cortex and thalamus. Journal of neurophysiology 100:1740-1748 doi:10.1152/jn.90463.2008

Zhang Y, Brady M, Smith S (2001) Segmentation of brain MR images through a hidden Markov random field model and the expectation-maximization algorithm. IEEE transactions on medical imaging 20:45-57 doi:10.1109/42.906424

Zvorykin VP (1980) [New data on individual quantitative features of the human lateral geniculate body]. Arkhiv anatomii, gistologii i embriologii 78:24-27

Figure 1
Click here to download high resolution image

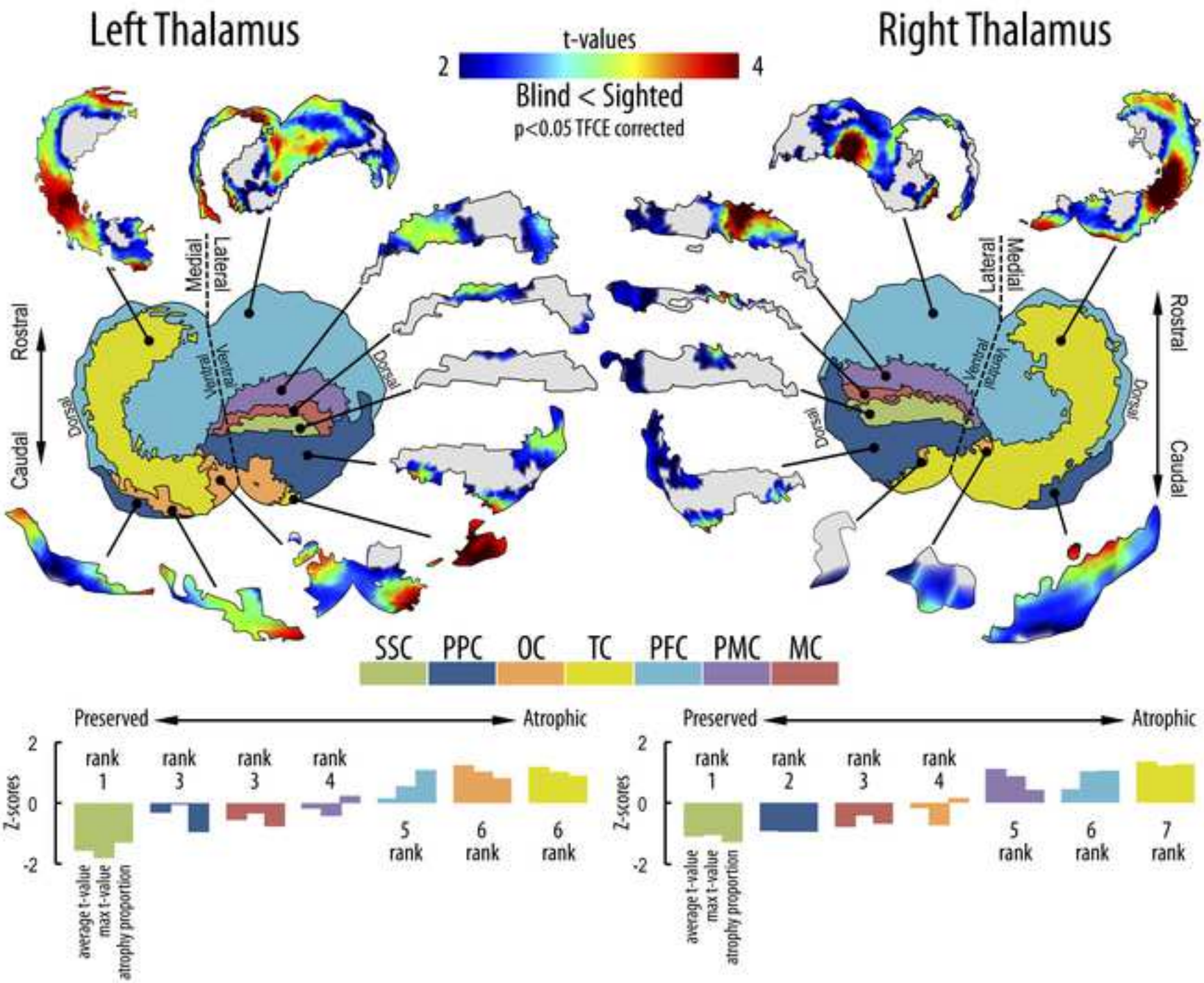

Figure 2
Click here to download high resolution image

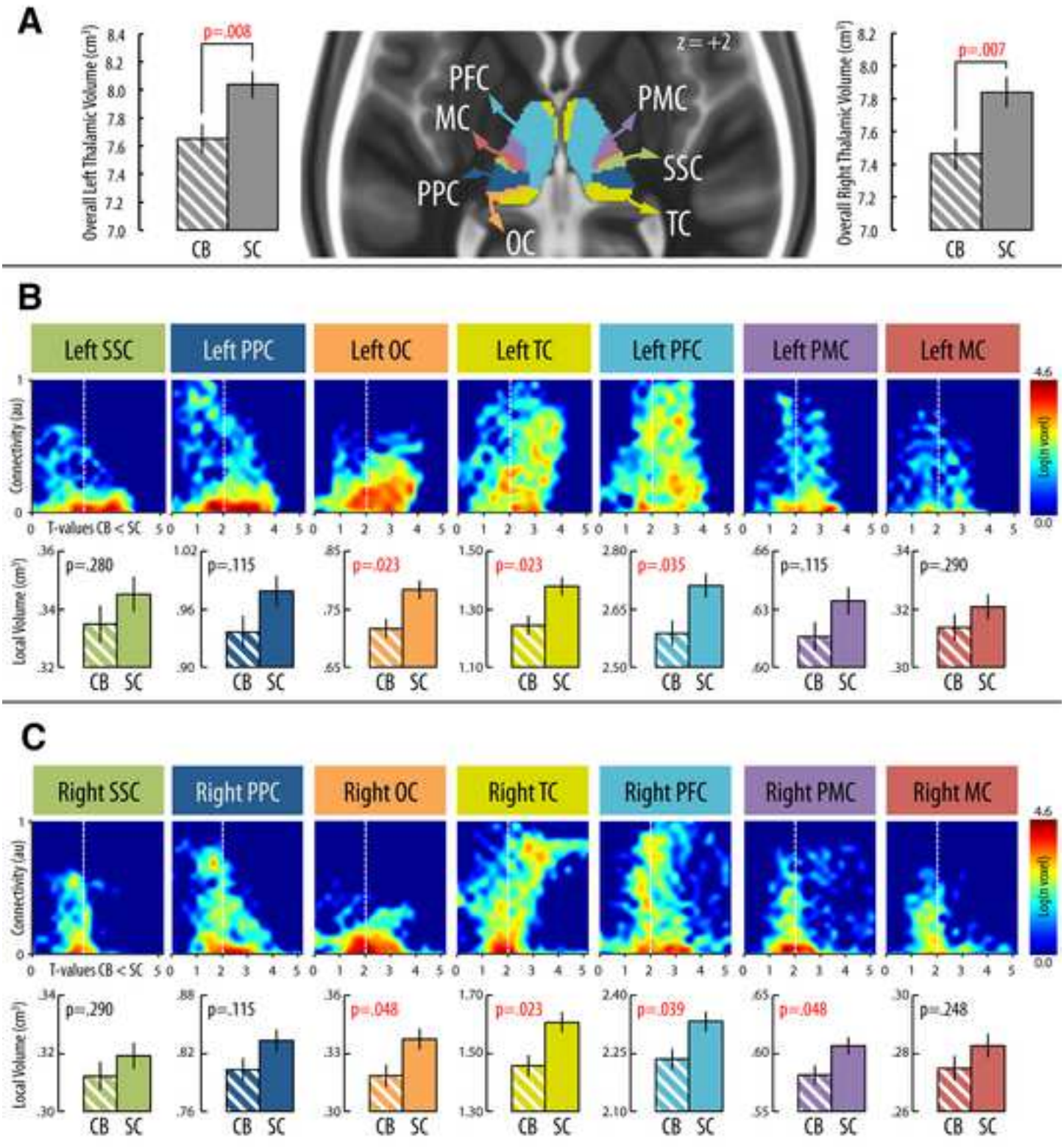

Figure 3
Click here to download high resolution image

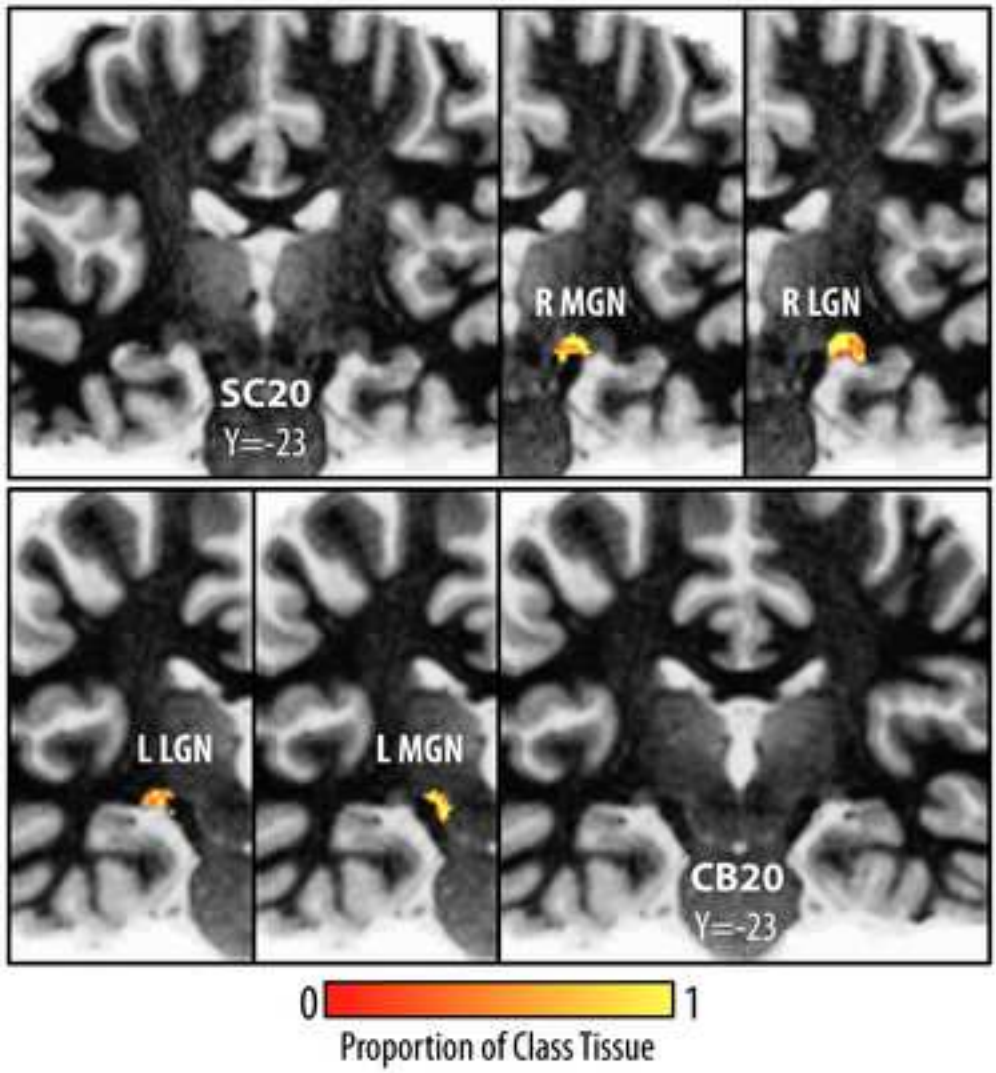

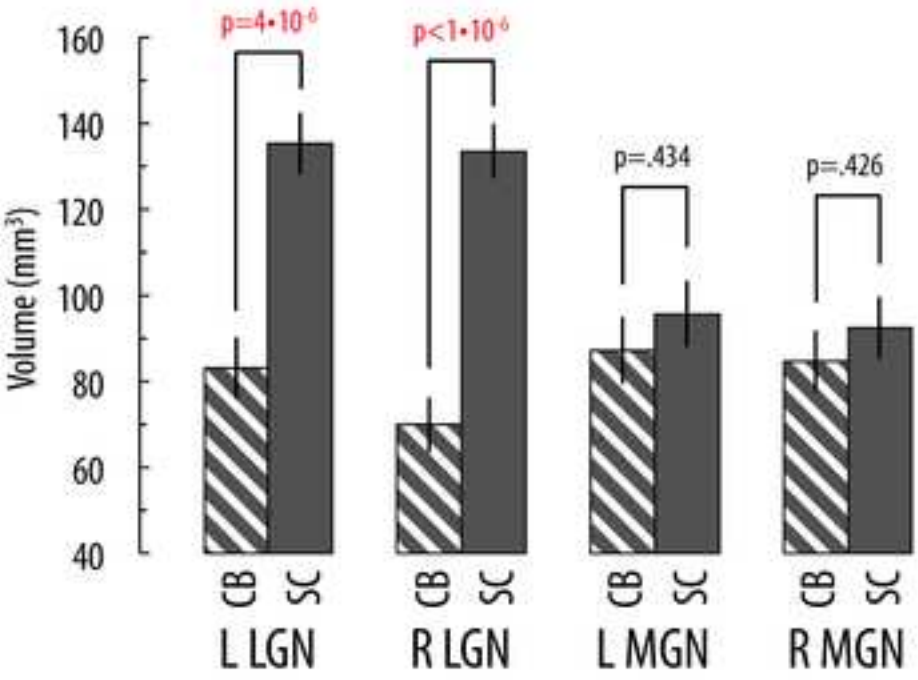

Figure 4
Click here to download high resolution image

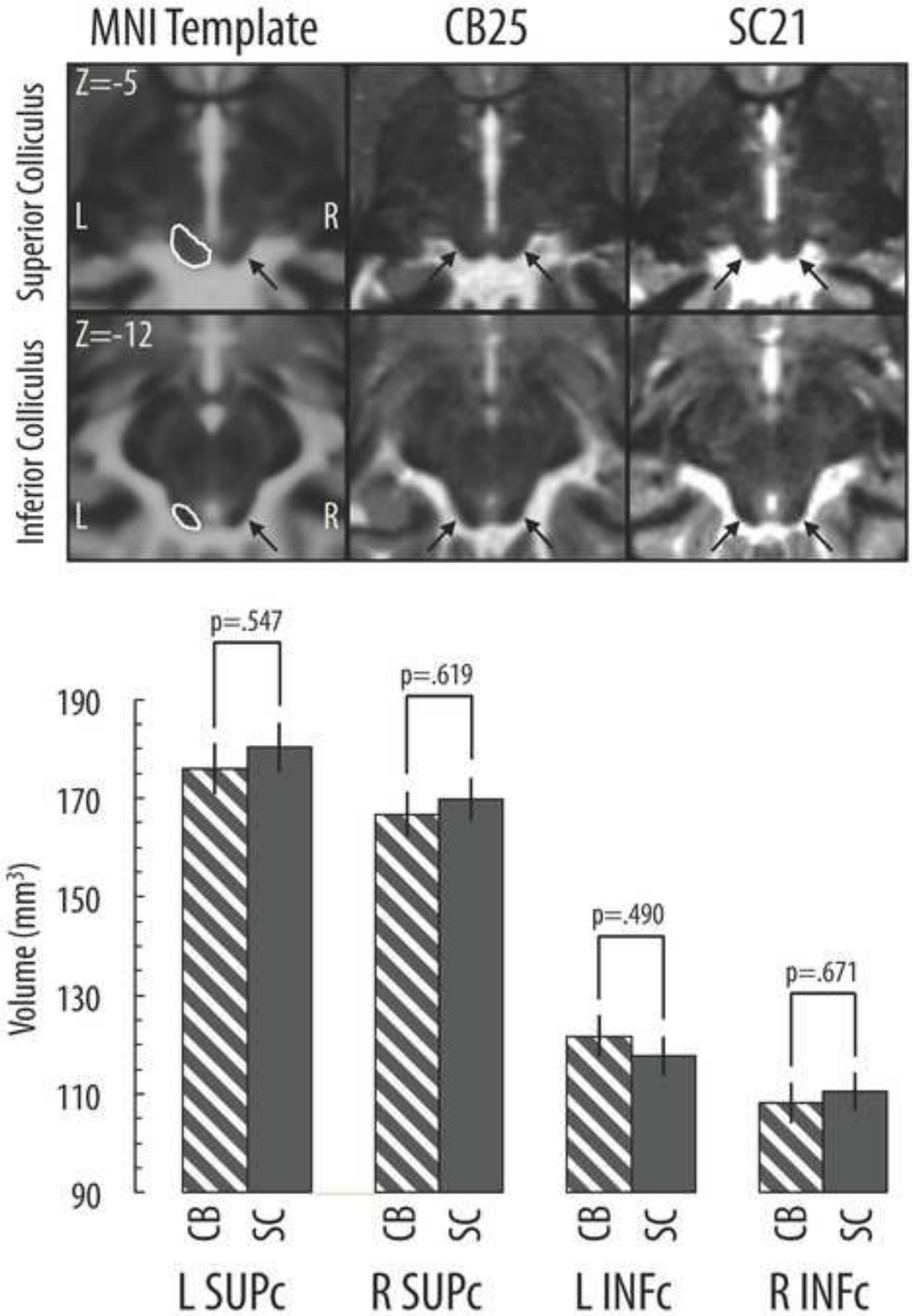

Table 1: Demographic and anamnestic data for the CB participants

Subjects				Characteristics of blindness	
ID	*Gender*	*Age*	*Hand,*	*Cause*	*Onset*
CB01	F	49	R	Retinopathy of prematurity	Birth
CB02	M	41	R	Retinis pigmentosa	Birth
CB03	M	39	R	Retinal detachment	Birth
CB04	M	58	R	Congenital cataract	Birth
CB05	M	38	R	Retinopathy of prematurity	Birth
CB06	F	31	R	Glaucoma, aniridia	Birth
CB07	M	20	R	Leber's amaurosis	Birth
CB08	M	23	R	Congenital cataract	Birth
CB09	M	27	R	Fibroblasia	Birth
CB10	F	27	R	Optic nerve atropy	Birth
CB11	F	42	R	Retinopathy of prematurity	Birth
CB12	M	60	R	Congenital glaucoma	Birth
CB13	F	31	R	Microphthalmia + Congenital Cataract	Birth
CB14	F	23	R	Optic nerve atropy	Birth
CB15	M	35	R	Retinopathy of prematurity	Birth
CB16	M	57	R	Congenital cataract	Birth
CB17	M	58	R	Congenital glaucoma	Birth
CB18	F	19	R	Congenital glaucoma	Birth
CB19	F	63	R	Congenital glaucoma	Birth
CB20	F	26	R	Retinopathy of prematurity	Birth
CB21	M	56	R	Retinopathy of prematurity	Birth
CB22	F	21	R	Retinopathy of prematurity	Birth
CB23	M	21	R	Retinopathy of prematurity	Birth
CB24	F	41	R	Retinopathy of prematurity	Birth
CB25	M	19	R	Retinopathy of prematurity	Birth
CB26	M	23	L	Retinopathy of prematurity	Birth
CB27	F	27	R	Retinopathy of prematurity	Birth
CB28	M	35	R	Unknown	Birth
CB29	M	23	R	Glaucoma	Birth

Table 2: Cortical projections of thalamic nuclei, in accordance to Behrens et al., 2003

Thalamic Nuclei	Projecting to
Lateral Posterior (LP); Ventral Posterolateral (VPL); Ventral Posteromedial (VPM)	Somatosensory Cortex (SSC)
Anterior Pulvinar	Posterior Parietal Cortex (PPC)
Inferior Pulvinar; Intralaminar	Occipital Cortex (OC)
Medial Pulvinar; Inferior Pulvinar; Mediodorsal (MD); Anterior Complex (AC)	Temporal Cortex (TC)
Mediodorsal (MD); Ventral Anterior (VA); Anteromedial (AM); Anterodorsal (AD)	Prefrontal Cortex (PFC)
Anterior part of the Ventral Lateral (VLa); Posterior part of the Ventral Anterior (VAp)	Premotor Cortex (PMC)
Posterior part of the Ventral Lateral (VLp)	Primary motor Cortex (MC)

Congenital Blindness affects Diencephalic but not Mesencephalic Structures in the Human Brain

Journal: Brain Structure and Function

Luca Cecchetti[1,2], Emiliano Ricciardi[1], Giacomo Handjaras[1,2],
Ron Kupers[3], Maurice Ptito[3,4,5] and Pietro Pietrini[1,2]

1 - Laboratory of Clinical Biochemistry and Molecular Biology, Department of Surgery, Medical, Molecular Pathology, and Critical Area, University of Pisa, Pisa, Italy;
2 - Clinical Psychology Branch, Pisa University Hospital, Pisa, Italy;
3 - BRAINlab and Neuropsychiatry Laboratory, Department of Neuroscience & Pharmacology, Panum Institute, University of Copenhagen, Copenhagen, Denmark;
4 - Harland Sanders Chair, School of Optometry, University of Montreal, Montreal, Canada;
5 - Laboratory of Neuropsychiatry, Psychiatric Centre Copenhagen and Department of Neuroscience and Pharmacology, University of Copenhagen, Copenhagen, Denmark;

Running Title: The subcortical blind brain

Correspondence to:
Emiliano Ricciardi
Laboratory of Clinical Biochemistry and Molecular Biology
Department of Surgical, Medical and Molecular Pathology and Critical Area
University of Pisa
Building 43, Via Savi 10, 56126, Pisa, Italy
E-mail: emiliano.ricciardi@bioclinica.unipi.it

Supplementary Material

Methods for the Whole Brain Voxel Based Morphometry Analysis and Validation of the Multicenter Sample

In order to test the validity of our multicenter sample and to subsequently permit a more detailed analysis of the thalamus, a whole-brain voxel based morphometry (VBM) was performed using SPM8 and the results were compared with those available from the literature. Thus, we used a mixture of Gaussian models and tissue probability maps (Ashburner and Friston, 2005) to automatically segment the cerebrospinal fluid (CSF), the white (WM) and grey matter (GM). Then, the diffeomorphic registration algorithm DARTEL (Ashburner, 2007) was implemented pooling together the probability maps of blind and sighted subjects (n=58), to obtain a 1.5 mm^3 study specific common template. In addition, the resulting images were transformed to match the MNI space, by means of an affine registration. The Jacobian determinants of the deformation were multiplied by the probability maps to ensure that the amount of GM and WM within each voxel was maintained after the registration (Good et al., 2001). Finally, a Gaussian spatial smoothing with a full width at half maximum (FWHM) of 4 mm was applied to the GM and WM partitions. Brain regions showing statistically significant differences between groups were determined using a univariate general linear model (GLM) that included age, scanner site, gender and overall brain volume (the sum of GM, WM and CSF voxels) as nuisance variables. Results were corrected for multiple comparisons using a single-voxel threshold of $p<0.01$ with a cluster extent of $p<0.05$ (family wise error corrected - FWEc) and were displayed on a inflated three-dimensional mesh of the brain using Caret v5.65 (Van Essen et al., 2001).

Results for the Whole Brain Voxel Based Morphometry Analysis and Validation of the Multicenter Sample

Whole brain VBM results showed that CB had a significant ($p<0.05$ FWEc) GM density reductions in the bilateral intracalcarine and cuneus cortex, parieto-occipital sulcus, lingual gyrus, and the anterior portion of the right superior and middle temporal gyri (Supplementary Fig. 1A and Supplementary Table 1). On the other hand, blind individuals showed an increased GM density in the subiculum and cornu ammonis of the right hippocampus, bilateral fusiform gyrus, right cerebellar lobule VI, left cerebellar crus I, right superior and middle frontal gyri (Supplementary Fig. 1A and Supplementary Table 1).

Analysis of WM changes revealed that CB participants had significant volumetric reductions of the bilateral optic tract, the retrolenticular part of the internal capsule, the optic radiations, forceps major, inferior longitudinal and left fronto-occipital fasciculi, and the splenium of the corpus callosum (Supplementary Fig. 1B and Supplementary Table 1). No regions showed a WM density increase for CB, as compared to SC.

Supplementary Figure 1 and Supplementary Table 1 about here

Discussion for the Whole Brain Voxel Based Morphometry Analysis and Validation of the Multicenter Sample

Compared to previous observations in blind individuals, the whole brain VBM analysis demonstrates a characteristic pattern of atrophy affecting both the white and grey matter of blind participants, mainly in vision-related brain structures. Significant density reductions in the white matter fasciculi are in agreement with those previously

reported in other studies (Shimony et al., 2006; Pan et al., 2007; Ptito et al., 2008) and were located in bilateral optic tract, retrolenticular part of the internal capsule, optic radiations, forceps major, inferior longitudinal and left fronto-occipital fasciculi, as well as the splenium of the corpus callosum. Consistently, comparisons in GM density described a significant reduction in the primary visual cortex, the cuneus, the parieto-occipital sulcus, the lingual gyrus and the anterior portion of the right superior as well as middle temporal gyri of CB (Noppeney et al., 2005; Ptito et al., 2008; Bridge et al., 2009). On the other hand, we found an increased GM in frontal regions and right hippocampus of CB, still in agreement to what has been reported in previous VBM studies (Noppeney et al., 2005; Fortin et al., 2008; Leporé et al., 2009).

Taken together, the overlap between our findings and those present in the literature could be considered a robust validation of our multicentric sample, supporting our observations for the visual and non-visual thalamic structures.

Methods for the volume estimation of the Superior and Inferior Colliculi using the MNI Standard Symmetric Template

Since only few studies (Kang et al., 2008; Sabanciogullari et al., 2013) used in-vivo techniques to investigate the absolute volume of the human superior and inferior colliculi, we provided a further validation for the results obtained in our multicentric sample. Therefore, we used an independent methodology to measure the volume of these mesencephalic structures in the MNI152 0.5mm Standard Symmetric Template (Fonov et al., 2009), aiming to produce an estimation of the tectum size for the reference population. Alternatively to the slice-by-slice ROI definition used in our sample, in this case we took advantage of the ellipsoidal shape of both the superior and inferior colliculi, to compute the volume as:

$$V = \frac{4}{3}\pi ABC$$

where A, B and C are the three orthogonal semi-axis of the ellipsoid.

Thus, one of the authors who was blind to the results obtained for the sighted and blind individuals and who was not involved in the volume estimation of the multicentric sample, measured accurately the three semi-axis of the superior and inferior colliculus for the MNI Template. As a first step of the procedure, the Template was rotated by 37° on the y-dimension so as the longest axis of the inferior colliculus was orthogonal to the horizontal plane (Supplementary Fig.2). This operation facilitated the definition of the three orthogonal axis of the colliculi. Similarly to Sabanciogullari and colleagues (2013), once both the superior and inferior colliculi were identified on a single sagittal plane, two of the three measures of interest (ventrodorsal and rostrocaudal axis) were obtained for each structure (m1, m2 for the inferior and m4, m5 for the superior colliculus). In addition, the third measure was defined on the transverse plane (lateromedial axis), respectively m3 for the inferior colliculus and m6 for the superior.

Moreover, A, B and C were defined for each structure as the half of m1, m2 and m3 for the inferior colliculus, as well as the half of m4, m5 and m6 for the superior colliculus and the absolute volumes were computed.

Lastly the volumes obtained for the MNI Template were compared to those of the sighted controls included in our study by means of a one-sample Z Test ($p<0.05$).

Results for the volume estimation of the Superior and Inferior Colliculi using the MNI Standard Symmetric Template

No statistically significant differences were found between the volume for the superior and inferior colliculus of the MNI 0.5mm Standard Symmetric Template as compared to those of the sighted controls included in the multicentric sample [Left Superior Colliculus: Z-score = -0.318; p-value = 0.750. Right Superior Colliculus: Z-score = 0.085; p-value = 0.932. Left Inferior Colliculus: Z-score = -0.707; p-value = 0.480. Right Inferior Colliculus: Z-Score = -0.387; p-value = 0.699]. Specifically, this independent estimation of the tectum size produced 6.5 mm, 5.05 mm and 5.96 mm respectively for the ventrodorsal, rostrocaudal and lateromedial axis of the inferior colliculus as well as an absolute volume of 102.48 mm^3. On the other hand, for the superior colliculus we obtained an absolute volume of 171.82 mm^3 and a length for the ventrodorsal, rostrocaudal and lateromedial axis of 4.81 mm, 9.41 mm and 7.25 mm, respectively.

Taken together, the agreement between the independent assessment for the tectum size of the MNI Template, the values reported for sighted individuals included in our study and the volumes described by previous studies (Kang et al., 2008; Sabanciogullari et al., 2013) provided a valuable validation for the methodology used in volumetric analysis of colliculi.

Figure Legends

Supplementary Fig.1 Results for grey (A) and white (B) matter VBM analyses, while comparing CB and SC. Brain regions showing significant GM and WM reductions in CB are represented in red and yellow ($p<0.05$ FWEc), whilst GM reductions for SC are displayed in blue and cyan, using the same statistical threshold. We found no significant reductions in WM of sighted compared to blind individuals. Calcarine (CalS), collateral (ColS), parieto-occipital (POS), cingulate (CingS), superior temporal (STS) and superior frontal (SFS) sulci are shown as white dashed lines to easily allow the localization of significant clusters (Fig.1A). In panel 2B, the inferior longitudinal fasciculus (ILF), the optic tract (OptT) and radiations (OptR), the retrolenticular part of the internal capsule (IC), the splenium of the corpus callosum (Spl) and the forceps major (FoM) are highlighted by black arrows

Supplementary Fig.2 Methodology used to measure the three orthogonal axis of the superior and inferior colliculi. Specifically, the ventrodorsal and rostrocaudal axis were defined on the same sagittal slice for both the inferior (m1, m2) and the superior colliculus (m4, m5), whereas the lateromedial axis was defined on two different axial slices: m3 on slice “a” for the inferior colliculus and m6 on slice “b” for the superior.

Supplementary Table 1: Grey and white matter VBM results

Grey matter VBM analysis: SC > CB

Cluster Level			Voxel Level				
ID	p FWEc	k	T-value	x	y	z	Label
1	0.000	13445	4.155	-5	-76	10	Left Intracalcarine Cortex
			3.954	10	-67	13	Right Intracalcarine Cortex
			3.305	-11	-66	22	Left Parieto-Occipital Sulcus
			2.493	11	-65	22	Right Parieto-Occipital Sulcus
			4.744	-11	-62	3	Left Lingual Gyrus
			4.182	14	-56	4	Right Lingual Gyrus
2	0.006	2801	3.864	55	-5	-16	Right Superior Temporal Sulcus
			3.645	62	0	-21	Right Middle Temporal Gyrus
			2.622	53	-13	-7	Right Superior Temporal Gyrus

Grey matter VBM analysis: CB > SC

Cluster Level			Voxel Level				
ID	p FWEc	k	T-value	x	y	z	Label
1	0.000	5640	5.196	39	-49	-20	Right Fusiform Gyrus
			3.105	22	-29	-11	Right Hippocampus (Subiculum)
			2.756	24	-14	-11	Right Hippocampus (Cornu Ammonis)
			4.154	36	-60	-23	Right Cerebellar VI
2	0.001	4264	4.812	-40	-75	-23	Left Cerebellar Crus I
			3.942	-36	-71	-19	Left Fusiform Gyrus (occipital portion)
			3.061	-27	-41	-20	Left Fusiform Gyrus (temporal portion)
3	0.012	2732	4.431	10	49	43	Right Superior Frontal Gyrus
			3.747	22	39	39	Right Superior Frontal Sulcus
4	0.033	2297	3.638	28	49	20	Right Middle Frontal Gyrus
			3.475	22	62	18	Right Frontal Pole

White matter VBM analysis: SC > CB

Cluster Level			Voxel Level				
ID	p FWEc	k	T-value	x	y	z	Label
1	0.000	55358	5.172	0	-36	13	Splenium of the Corpus Callosum
			3.477	23	-51	15	Right Forceps Major
			3.475	-18	-51	12	Left Forceps Major
			8.250	-28	-63	15	Left Optic Radiation
			6.536	31	-59	17	Right Optic Radiation
			3.404	-43	-36	-11	Left Inferior Longitudinal Fascisulus
			3.779	41	-38	-8	Right Inferior Longitudinal Fasciculus
			3.413	36	-31	4	Right Retrolenticular part of IC
			7.965	16	-7	-11	Right Optic Tract
2	0.004	5780	8.302	-12	-5	-12	Left Optic Tract
			3.093	-35	-10	-12	Left Inferior Fronto-Occipital Fasciculus
			3.619	-24	-24	2	Left Retrolenticular part of IC

Supplementary Material Figure 1
Click here to download high resolution image

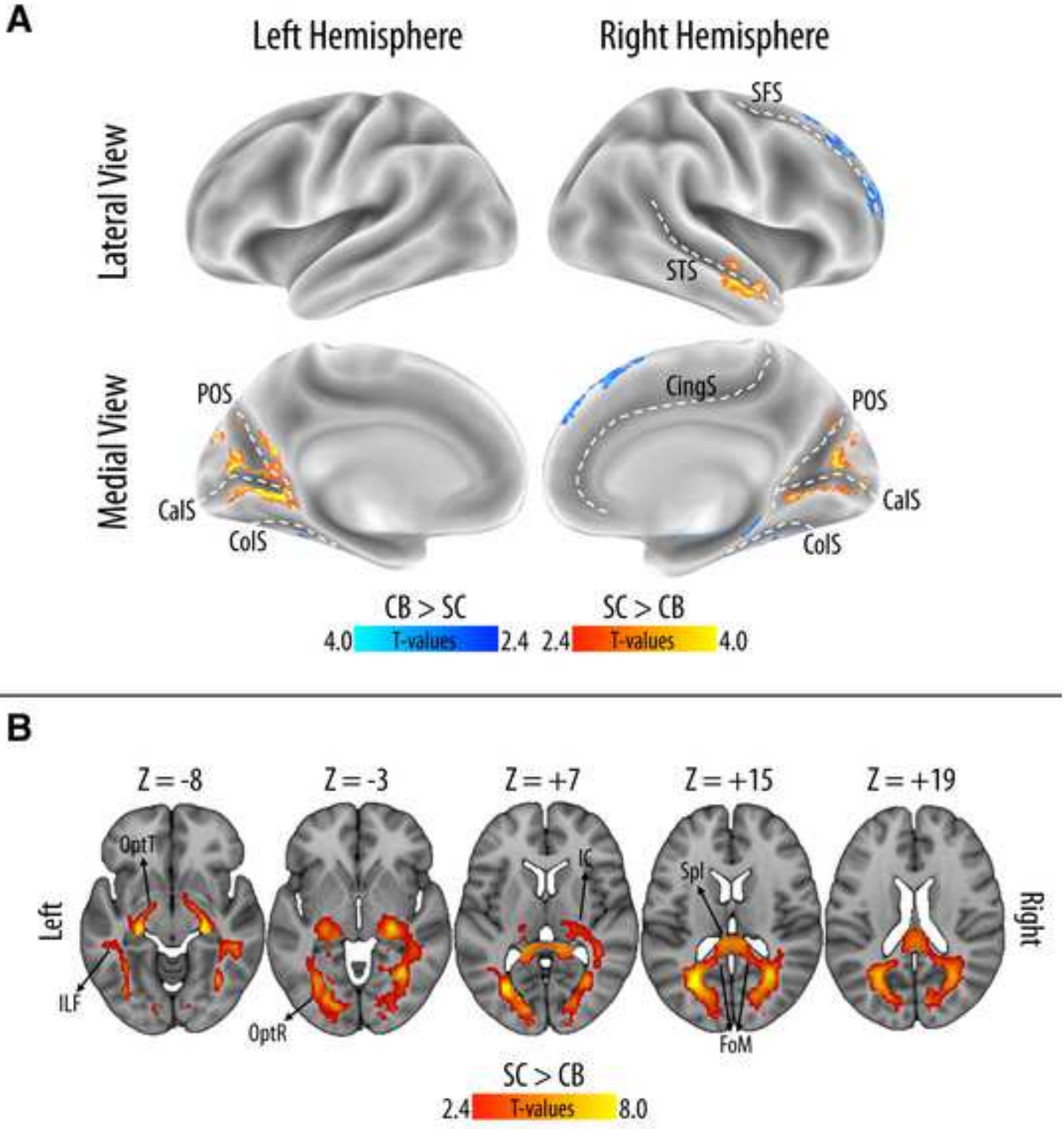

Supplementary Material Figure 2
Click here to download high resolution image